Journal of Human Evolution 202 (2025) 103665

Contents lists available at ScienceDirect

Journal of Human Evolution

journal homepage: www.elsevier.com/locate/jhevol

Aurignacian groups at Isturitz (France) adapted to a shifting environment upon their arrival in Western Europe ~42,000 years ago

E. Berlioz [a], M. Fernández-García [b, c], M.-C. Soulier [d], L. Agudo-Pérez [a], G. Amorós [e], C. Normand [d], A.B. Marín-Arroyo [a, *]

[a] Research Group I+D+i EvoAdapta (Evolución Humana y Adaptaciones durante La Prehistoria), Department of Historical Sciences, University of Cantabria, Santander, 39005, Spain
[b] Departament de Prehistòria, Arqueologia i Història Antiga, Universitat de València, Valencia, 46010, Spain
[c] IPHES-CERCA (Institut Català de Paleoecologia Humana i Evolució Social), Tarragona, 43007, Spain
[d] Laboratoire TRACES, UMR 5608, CNRS, Université de Toulouse-Jean Jaurès, F-31058, Toulouse Cedex 9, France
[e] Research Group ECCE HOMO (Evolución, Cenozoico, Cuaternario, Ecología HOMO), Department of Plant Biology, Faculty of Biology, University of Murcia, Murcia, 30003, Spain

ARTICLE INFO

Article history:
Received 22 July 2024
Accepted 17 February 2025
Available online xxx

Handling Editor: Dr N Sala

Keywords:
Early Upper Paleolithic
Paleoenvironments
Stable isotopes
Collagen
Dental enamel
3D-Dental microwear texture analysis

ABSTRACT

The Marine Isotope Stage 3 is a context of considerable climatic instability. Establishing the link between global climate changes and their impact on the local ecological contexts and prey exploited by human populations is challenging. Still, it is necessary to understand better the local conditions where humans lived to unravel how they adapted to fluctuating environmental conditions. Here, we address this question by studying 250 osteodental elements from animals hunted and consumed by human groups at Isturitz, a rich and well-documented French archaeological site and one of the earliest in Western Europe where the Aurignacian technoculture has been attested. To do so, we set up a multiproxy approach (archaeozoology, three-dimensional dental microwear texture analyses, and stable isotopic analyses of $\delta^{18}O$ and $\delta^{13}C$ in enamel bioapatite and $\delta^{13}C$, $\delta^{15}N$, and $\delta^{34}S$ in bone collagen) that informs us on a timeline from the first years to the last few days of an animal's life. We reconstructed their ecologies and paleoenvironments during the different Aurignacian phases at Isturitz. Our findings indicate that the first human occupations at Isturitz occurred under cold and arid conditions, rapidly becoming even cooler and drier. Limited changes are observed in the human-environment-prey relationship despite this unstable climatic context where significant changes in rainfall, temperature, and a gradual opening of environments and some changes in the faunal assemblage occurred. Our findings suggest that human groups hunted in similar territories and utilized comparable strategies throughout the temporal sequence. Our multiproxy approach, combining complementary analyses, provides a better understanding of the adaptation strategies when the first phases of the Upper Paleolithic were emerging in Western Europe.

1. Introduction

The Marine Isotope Stage 3 (MIS3: 57–27 ka cal BP) was a period of considerable climatic instability, characterized by rapid and abrupt oscillations on a scale of hundreds to thousands of years, alternating cold and temperate climatic events (Lisiecki and Raymo, 2005; Gibbard and Cohen, 2008; Sánchez Goñi et al., 2008; Wolff et al., 2010). These global climatic changes resulted in multiple and profound modifications to the ecosystems (Vidal-Cordasco et al., 2022, 2023), forcing flora and human and nonhuman fauna to constantly adapt, as reflected by vegetation changes (Fourcade et al., 2022) and faunal turnovers (Discamps et al., 2011). However, it remains difficult to establish a straightforward relationship between these global climate changes and their regional and local impact on the ecology of human populations and their exploited prey.

The MIS3, at the Middle to Upper Paleolithic transition, coincides in Europe with the progressive decline of late Neanderthal

* Corresponding author.
E-mail address: anabelen.marin@unican.es (A.B. Marín-Arroyo).

https://doi.org/10.1016/j.jhevol.2025.103665

groups until their final diminish and the arrival of the first wave of *Homo sapiens*. The Aurignacian technocomplex and its technical innovations have been, until recently, widely accepted as one of the first industries associated with the arrival of *H. sapiens* in Europe (Mellars, 2006 and references within). However, recent evidence from ancient DNA has shown interbreeding between modern humans, Denisovans, and Neanderthals (Sankararaman et al., 2012; Slon et al., 2018; Iasi et al., 2024), uncorrelated with variations in the lithic technocomplexes. It provides a more complex picture of this transitional period (Slimak et al., 2022; Hublin et al., 2020; Mylopotamitaki et al., 2024) and underlines the need for extensive genetic studies (e.g., Hajdinjak et al., 2021; Prüfer et al., 2021). The Isturitz cave (French Basque Country—Fig. 1A) is one of the few sites where Proto-Aurignacian and Early Aurignacian technocomplexes are found on stratigraphy (Normand et al., 2007). Isturitz is strategically located at the crossroads of the Pyrenees, the Aquitaine Basin, and the Vasco-Cantabrian area, three regions sharing numerous contemporaneous cultural similarities (Normand, 2005; Rendu et al., 2017). As a result, Isturitz is a key archaeological site for evaluating the local effects of global climatic changes on plant and animal populations and, therefore, on the ecological setting exploited by Aurignacian human populations. In this study, we decipher the impact of MIS3 climate oscillations on the local ecological and environmental conditions faced by human groups at Isturitz and how they adapted their subsistence strategies to them. The recent excavations, based on a more meticulous and integral process with modern analytical methods, enable us to address these particular issues on a fine scale due to the multiple stratigraphic layers precisely dated (Normand et al., 2007; Soulier, 2013; Rendu et al., 2017; Barshay-Szmidt et al., 2018). Our study

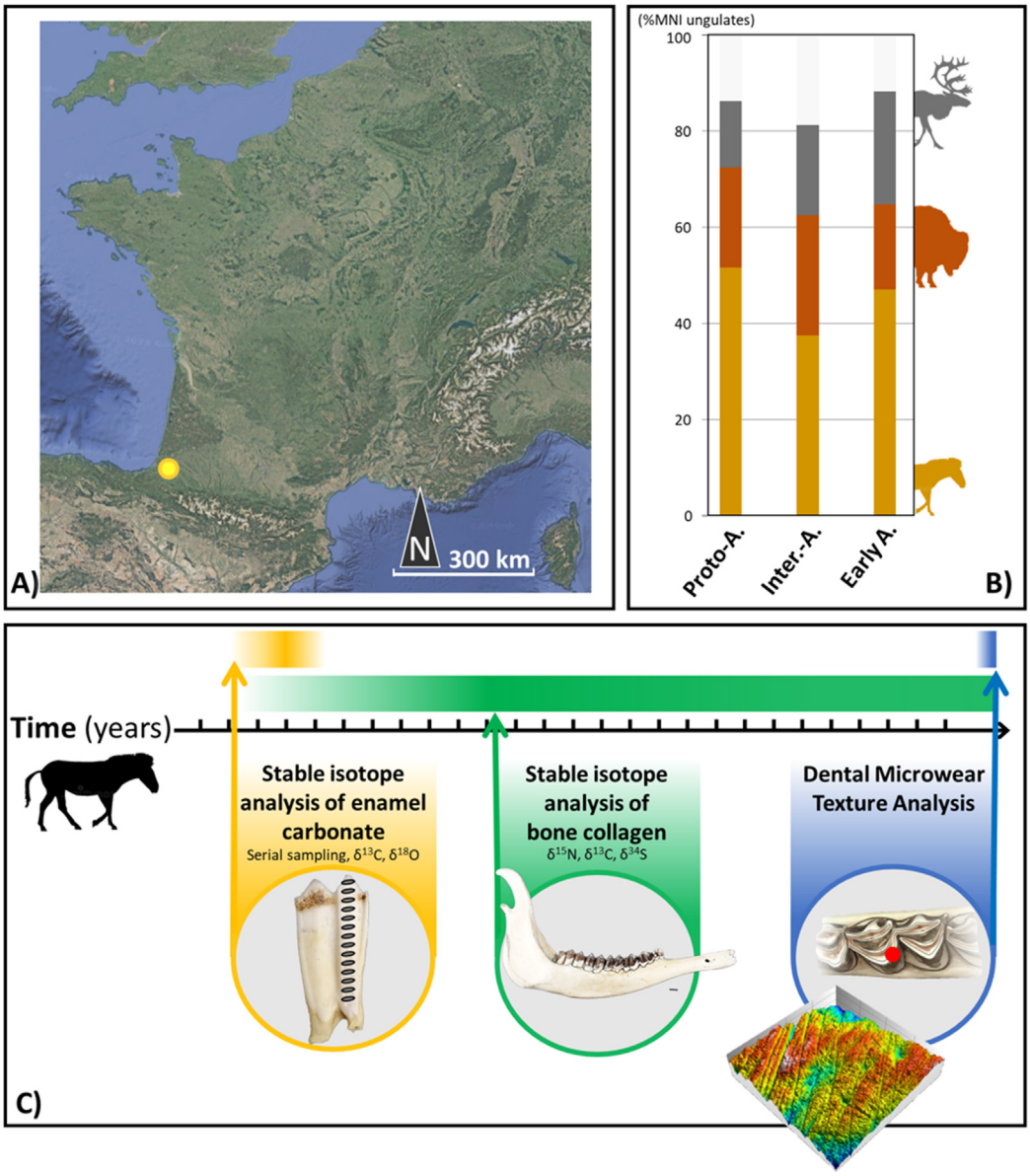

Figure 1. A) Location of the Isturitz cave in southwestern France (maps taken from earth.google.com). B) Proportion of the three main prey at Isturitz out of the total number of ungulates, calculated from the maximum MNI (Minimum Number of Individuals) for each taxon (data taken from table 3.4.1. of Soulier, 2013). C) Three combined proxies provide complementary time scales of animal life (early years for stable isotope analysis of enamel carbonate; late >10 years for stable isotope analysis of bone collagen and last weeks of the life for dental microwear texture analysis) that allow the reconstruction of the ecology and habitat of ungulates exploited by human populations at Isturitz. (For interpretation of the references to color in this figure, the reader is referred to the Web version of this article.)

focused on ungulate bones and teeth of animals hunted and consumed by the human groups that occupied Isturitz during the Aurignacian, as well as some carnivore bones that allowed us to identify their role in food webs. To obtain a comprehensive overview of early human ecological conditions in Isturitz, we combined, on the same specimens, three informative proxies at complementary temporal scales which provide information on the ecosystems and living conditions of animals from their earliest years (stable isotope analysis from horse dental enamel and bone collagen on both ungulates and carnivores) to the last few weeks before death (dental microwear texture analysis [DMTA] of ungulates). This approach enabled us to explore the complementary life-history traits of these animals across their entire lifespan. We also provided a revised chronology of the Isturitz human occupation phases. One of the strengths of this approach is the combination of stable isotopic analysis on mammal bones and teeth and DMTA, an approach still seldom applied in archaeological contexts to date.

We hypothesized that the landscape evolution around Isturitz induced by global climate change during the MIS3 led herbivores to progressively modify their feeding behavior and habitat use in response to variations in resource availability and living conditions. In turn, changes in landscapes and prey behavior were expected to modify human hunting territories and alter subsistence strategies to continue meeting their nutritional needs. We expected to find a correlation between changes in lithic production related to the human subsistence strategies adopted over time and, thus, an evolution of ecosystems during the development of the earliest Upper Paleolithic.

By unraveling hominin procurement strategies, hunting decisions, and behavior, our study documents the temporal evolution of the human-environment-prey relationship under changing climatic and environmental conditions when the makers of the Aurignacian technocomplex occupied the Isturitz cave and exploited its surroundings.

2. Materials and methods

2.1. Archaeological site: Isturitz

The Isturitz cave system, situated in the valley of the river l'Arberoue in France (Western Pyrenees; Fig. 1A), is a relevant archaeological site attesting to the earliest evidence of Aurignacian in Western Europe. This karstic system was formed by the river flowing through the hill made of Aptian limestone (Normand, 2005; Lenoble and Texier, 2016). The galleries Isturitz and Saint-Martin of the Isturitz cave were excavated from 1912 onward (Passemard, 1913; De Saint-Périer, 1935; Normand, 2005). They preserve a long stratigraphic sequence from the Mousterian to the Bronze Age (Normand et al., 2007), including several levels corresponding to the different phases of the Aurignacian occupation, located in the lithostratigraphic unit III, sedimentary deposits of which were formed by runoff and rockfall processes (Normand, 2005). These levels yielded well-preserved archaeological material, including abundant lithics and bone tool industry (Tarriño and Normand, 2002; Normand et al., 2007), ornaments (White and Normand, 2015), as well as thousands of faunal skeletal remains (more than 11,000 for recent excavations; Soulier, 2013). Recent excavations took place in three sectors, respectively, named 'Principal excavation,' 'Profile,' and 'Extension' within the Galerie Saint-Martin, which presents a succession of archaeological levels documenting the different Aurignacian phases. These levels are grouped into three archaeostratigraphic units representing, based on their lithic and bone technocomplexes, the Proto-Aurignacian (C 4c6 to 12 and C 4d1 from the Principal excavation and C 4III from the Profile; Normand, 2005; Normand et al., 2007; Soulier, 2013), the Intermediate Aurignacian (C 4c4 and C 4c5 from the 'Principal excavation,' C 4II from the 'Profile,' and E 4Ic from the 'Extension'), and the Early Aurignacian (layers C 4b1 and C 4b2 from the 'Principal excavation,' C 4Ia and C 4Ib from the 'Profile,' and E 4Ia and E4Ib from the 'Extension'). The term 'Intermediate' (Normand, 2005) refers solely to the position of the archaeostratigraphic unit in the stratigraphy; it has no evolutionary significance. This level, however, presents singularities in terms of taphonomy and faunal assemblage that seem to exclude the possibility of representing a mixture between the overlying Proto-Aurignacian and the underlying Early Aurignacian (Soulier, 2013). A recent chronological study (Barshay-Szmidt et al., 2018) dated well-provenanced, species-identified, humanly modified faunal remains from the different archaeological layers of each Aurignacian variant. Results indicate they were accumulated very close in time to one another, with the Proto-Aurignacian starting at 42.8–41.3 ka modeled BP, the Intermediate Aurignacian at 42.2–41.1 ka modeled BP, and the Early Aurignacian at 41.6–39.7 ka modeled BP (for further information, see Normand, 2005, 2017; Normand et al., 2007; Soulier, 2013; Barshay-Szmidt et al., 2018 and references therein).

2.2. Faunal data

The study focuses on 51 mammal bones and 126 teeth of specimens recovered in the Aurignacian units from the Normand excavations in the Saint-Martin gallery (excavation sectors 'Principal excavation,' 'Profile,' and 'Extension'; Supplementary Online Material [SOM] Table S1). We included both ungulates, among which the bovines aurochs/bison (*Bos primigenius*/*Bison priscus*) ($N = 4$ teeth and 19 bones), horses (*Equus ferus*) ($N = 118$ teeth and 13 bones), and reindeer (*Rangifer tarandus*) ($N = 7$ teeth and 9 bones) were the more abundant, and carnivores, including foxes (*Vulpes* sp.) ($N = 6$ bones) and a bear (*Ursus* sp.; specimen IST64; SOM Tables S1 and S2). Twenty-eight additional specimens, including one hyena bone and eight bovine, 13 equid, three reindeer, and three fox bones, were analyzed but excluded from the interpretations because they did not meet the quality criteria for the isotope analysis on bone collagen (see SOM Table S2). The morphological similarity between the auroch and bison teeth did not allow us to clearly distinguish between these two species. For this reason, they were grouped as 'Bovines'. Although the ecology of these two species may differ, the literature supports a wide geographical distribution and range of habitats and feeding behavior for both bison (Guthrie, 1990; Stuart, 1991; Merceron and Madelaine, 2006; Rivals and Álvarez-Lao, 2018) and aurochs (Noe-Nygaard et al., 2005; Van Vuure, 2005; Helmer and Monchot, 2006; Wright, 2013), which supports a certain ecological plasticity for these large bovids. Archaeozoological and taphonomic study was previously completed by Soulier (2013). Due to the high fragmentation state, we conducted a zooarchaeology by mass spectrometry analysis for the bear specimen to confirm its taxonomic assignment following the methodology by Torres-Iglesias et al. (2024). All specimens are stored at the Centre Départemental d'Archéologie of Hasparren (France) and the UMR 5608 TRACES Lab (Toulouse, France).

The faunal assemblages in the three Aurignacian archaeostratigraphic units are dominated by the trio horse-bison-reindeer, with the horse being the most prevalent throughout the sequence (Soulier, 2013; Soulier et al., 2014) (Fig. 1B). Reindeer is the second most common taxon in the Early Aurignacian assemblage, while large bovids hold this position for the Proto-Aurignacian and Intermediate Aurignacian. Some carnivores (especially foxes) are also attested, but gnawing marks and digestion traces from carnivores are limited (<1.5%) compared to the extensive butchery marks documented (between 22% and 35% depending on the layers; table

2.4.2 in Soulier, 2013: refer to calculation details). The percentage of cutmarks is calculated from those elements with a well-preserved bone surface. The diversity of exploited species in the Proto-Aurignacian is more significant than in more recent archaeostratigraphic units, particularly for carnivores (Soulier, 2013). For all three assemblages, the seasonality data were obtained by archaeozoology and cementochronology. Results reveal horse hunting during the good season (from May to October) and reindeer hunting in the middle of the good season, covering the whole season from May to mid-December (Rendu et al., 2017). The study of fetal remains and decidual teeth completes this picture, illustrating winter hunting episodes in all three archaeostratigraphic units for horse, reindeer, and bison (Soulier, 2013).

2.3. Methods

Bayesian chronological model To establish a more precise timing for the Proto-Aurignacian, Intermediate Aurignacian, and Early Aurignacian archaeostratigraphic units of Isturitz, we relied on previously published radiocarbon dates (Barshay-Szmidt et al., 2018), which we calibrated with the IntCal20 calibration curve (Reimer et al., 2020). This curve is based on updated data, more accurate and robust than its previous version, IntCal13 (Reimer et al., 2013), available in 2018. A new Bayesian age model using the software OxCal v.4.4 (Bronk Ramsey, 2021) was done to recalculate the duration of the four studied phases. The code of the Bayesian chronological model is provided in SOM 1 (Supplementary information).

Three ecological proxies: three temporal scales We prioritized ungulate long bones of adult individuals (SOM Table S1) with evidence of human manipulation and ungulate teeth from units with attested anthropogenic activity. The anthropogenic origin of the assemblage was determined during the archaeozoological and taphonomic study (Soulier, 2013). From that information, firstly, stable isotopic tooth enamel values allow for the revealing of the environment during the mineralization of animal teeth (Balasse, 2003; Zazzo et al., 2012). In the case of the lower third molars of horses selected in this study, the enamel mineralization covers a time interval between 1 and 2 years and corresponds to the 21st to 55th months of life, corresponding to adult individuals and thus avoiding weaning signal on the recorded isotopic values (Hoppe et al., 2004; Fig. 1B). Secondly, we achieved stable isotope analysis on bone collagen, which reveals general information reflecting several years of an individual's life (the last 10 years or more, according to Hedges et al., 2007; Fig. 1B). And thirdly, DMTA allows us to characterize the diet of the last few weeks of the animal's life (Calandra and Merceron, 2016; DeSantis, 2016; Winkler et al., 2020; Fig. 1B). This multiproxy approach (Fig. 1C) offers a local reconstruction of the paleoenvironments exploited by human groups at Isturitz from the Proto-Aurignacian to the Early Aurignacian.

Stable isotope analysis of bioapatite ($\delta^{18}O_{carb}$ and $\delta^{13}C_{carb}$) As mammal body organic tissues grow, they retain the isotopic signature of local ecosystems at a particular time, revealing spatial isotopic variations. Here, we analyzed the stable isotopic values of $\delta^{13}C$ and $\delta^{18}O$ in the hydroxyapatite on the enamel carbonate. In intratooth sequential sampling, $\delta^{13}C$ isotopes measured in the carbonate fraction record seasonal changes in dietary behaviors and habitat use (Balasse et al., 2003; Palmqvist et al., 2003; Bernard et al., 2009). On the other hand, $\delta^{18}O$ mainly reflects the effect of temperature, as well as geographic factors such as latitude, altitude, and distance from the coast (Dansgaard, 1964; Bowen and Wilkinson, 2002; Ben-David and Flaherty, 2012; Clementz, 2012; Pederzani and Britton, 2019; Bataille et al., 2021). $\delta^{18}O_{carb}$ is directly related to the local meteoritic water ingested by animals via drinking water and feeding. Stable isotope analysis on enamel bioapatite was performed in a total of 11 lower third molars of *E. ferus* from the archaeostratigraphic units Proto-Aurignacian ($N = 5$), Intermediate Aurignacian ($N = 2$), and Early Aurignacian ($N = 4$; SOM Table S1). These teeth belong to at least nine different individuals, taking into account side, size, and use-wear during selection. Teeth were sequentially sampled with a low-revolution variable-speed manual drill in the EvoAdapta clean lab. Selected teeth are 4–6 cm long, allowing the collection of between 14 and 27 sequential subsamples, which are suitable for measuring at least one annual isotopic cycle. A total of 217 subsamples (10–15 mg) were taken on the labial side through stripes spaced 2–3 mm from the crown to the enamel root junction. $\delta^{18}O_{carb}$ and $\delta^{13}C_{carb}$ measurements were performed on carbonates from the untreated enamel powder at the Iso-Analytical Laboratory (Crewe, UK), using a continuous-flow isotope ratio mass spectrometer (Europa Scientific 20-20) coupled to a chromatograph. Sample pretreatment was not performed based on potential side effects. While pretreatment aims to remove organic matter and secondary carbonates from bioapatite, prior to stable isotope analysis, any method guarantees complete removal, and all of them can introduce undesirable alterations, particularly affecting $\delta^{18}O_{carb}$ values (Snoeck and Pellegrini, 2015; Pellegrini and Snoeck, 2016). Reference materials for Vienna Pee Dee Belemnite calibration and quality control standards were included. Sample replicates were included in every five samples. The analytical precision was better than 0.07‰ for $\delta^{13}C_{carb}$ and better than 0.11‰ for $\delta^{18}O_{carb}$ (see SOM S3 and SOM 6).

Air temperature and precipitation were estimated from $\delta^{18}O_{carb}$ and $\delta^{13}C_{carb}$, respectively (Pederzani et al., 2021; Fernández-García et al., 2023). On the one hand, mean annual precipitation (MAP) was calculated following the suggestion of Lécuyer et al. (2021). First, the $\delta^{13}C_{carb}$ is adjusted to the $\delta^{13}C$ obtained by the animal from the diet, using an enrichment factor of 13.7‰ that is specific to *E. ferus* (Cerling and Harris, 1999; Tejada-Lara et al., 2018). Subsequently, MAP estimation is based on the least square regression developed by Rey et al. (2013) and based on the dataset of Kohn (2004), which requires the estimation of $\delta^{13}C_{leaf}$. As noted by Lécuyer et al. (2021), these MAP estimates are preliminary and require validation with other proxies. On the other hand, temperatures were estimated from $\delta^{18}O_{carb}$ considering a two-step conversion. First, it was based on the linear regression between $\delta^{18}O_{carb}$ in tooth enamel and $\delta^{18}O$ in meteoric waters ($\delta^{18}O_{mw}$), created with modern datasets from horses and bovines (D'Angela and Longinelli, 1990; Bryant et al., 1994; Chillón et al., 1994; Huertas et al., 1995; Hoppe, 2006; Blumenthal et al., 2019). Subsequently, $\delta^{18}O_{mw}$ values were converted into temperatures considering the geographically adapted correlations proposed by Pederzani et al. (2021), based on European Global Network of Isotopes in Precipitation stations [International Atomic Energy Agency and the World Meteorological Organization] (see SOM S3 and SOM 6). The mean annual temperature (MAT) comes from the summer and winter averages from the unmodeled $\delta^{18}O_{carb}$ curve. The climatic estimates provided by this work should be considered exploratory due to the uncertainties associated with the calibrations (for further discussion, see Pryor et al., 2014; Lécuyer et al., 2021; Pederzani et al., 2023). Present-day temperatures and precipitation values were obtained from the WorldClim dataset v2 (Fick and Hijmans, 2017) based on the QGIS software. Data exploration and statistics were conducted with Excel and RStudio (v. 2023.03.1).

Stable isotope analysis of bone collagen ($\delta^{13}C_{coll}$, $\delta^{15}N_{coll}$, and $\delta^{34}S_{coll}$) Carbon stable isotope composition of organic tissues indicates the metabolic pathway of the plants eaten while the tooth was mineralizing (C3, C4, or Crassulacean acid metabolism). At that time, only C3 plants were present in European ecosystems. In modern ungulates, C3 feeders grazing in open environments have been shown to have higher $\delta^{13}C$ values than those occupying a

forested habitat due to differences in humidity, light exposition, and tree cover. This phenomenon is known as the 'canopy effect' (Drucker et al., 2008; Jones et al., 2021). Nitrogen stable isotope composition is used to determine the trophic position of animals (Drucker et al., 2003; Reade et al., 2023), but in terrestrial environments, nitrogen cycling is also influenced by abiotic factors, including temperature, precipitation, and altitude (Amundson et al., 2003; Männel et al., 2007; Craine et al., 2009), as well as by plant characteristics (Craine et al., 2009; Liu et al., 2010). Finally, sulfur stable isotope composition is strongly influenced by the local geological conditions and dry and wet deposition, including sea spray. It, therefore, provides information on the mobility of the specimens as it is influenced by the isotopic composition of the food consumed (Richards et al., 2003; Nehlich, 2015; Bataille et al., 2021).

For $\delta^{13}C$, $\delta^{15}N$, and $\delta^{34}S$ measured in bone collagen, we followed the procedure detailed in Jones et al. (2019). Bone samples were collected at the Centre Départemental d'Archéologie of Hasparren and TRACES Lab (France). Collagen was extracted following Brown et al. (1988) and Richards and Hedges (1999) at the EvoAdapta clean lab at the University of Cantabria (Santander, Spain). Stable isotopic measures were performed using a Europa Scientific 20-20 isotope ratio mass spectrometer at the Iso-Analytical Laboratory (Crewe, UK). Sample replicates were included in every five samples. Quality indicators for bone collagen were the following: % collagen (>1), %C (30–44%), %N (11–16%), %S (0.15–0.35%), C:N (2.9–3.6), C:S (600 ± 300), and N:S (200 ± 100) (DeNiro, 1985; Ambrose, 1990; Van Klinken, 1999; Nehlich and Richards, 2009). The $\delta^{13}C$, $\delta^{15}N$, and $\delta^{34}S$ values are reported relative to Vienna Pee Dee Belemnite, atmospheric air, and Vienna Canyon Diablo troilite (VCDT) standards, respectively.

When the number of individuals was ≥5, Kruskal-Wallis tests followed by Dunn's post hoc tests were carried out using RStudio v. 2023.03.1 Build 446 and the packages 'Hmisc,' 'corrplot,' 'onewaytests,' 'ggpubr,' 'ggplot2,' and 'magrittr' (Wickham et al., 2016; Dag et al., 2018; Harrell Jr and Harrell Jr, 2019; Wei et al., 2021; Bache et al., 2022; Kassambara, 2023). We provide the R Markdown file in SOM 2 (Supplementary information). In the case of small sample sizes (<5), we have not carried out any statistical tests, and only comments on the observed tendencies of these species in the 'Results' section are provided.

Three-dimensional dental microwear texture analysis The consumption of plants by primary consumers like herbivores induces micrometric scars on the occlusal enamel surface of dental facets (Ungar, 2015; Calandra and Merceron, 2016; DeSantis, 2016). These come in a variety of sizes and shapes. The resulting texture reflects the physical properties and inner composition of the animal diet (Grine, 1986; Teaford and Oyen, 1989; e.g., silica-bearing grasses, tough leaves, and seeds; Teaford and Glander, 1991; Scott et al., 2006; Ungar, 2015; Winkler et al., 2020) and has distinct characteristics depending on the proportion of silica-rich herbaceous plants, soft foliage, seeds, and fruits consumed (Calandra and Merceron, 2016). Therefore, there is a direct link between the animal and the vegetation available in its habitat, making it possible to draw inferences regarding the feeding ecology and the environment. As dental microwear textures are constantly changing as a result of continuous food intake, they characterize the diet of the last few weeks of an animal's life, which is known as the 'last supper effect' (Grine, 1986; Teaford and Oyen, 1989; Calandra and Merceron, 2016). It can, therefore, be used to highlight differences in diets between animals that die in different seasons (Merceron et al., 2010; Calandra et al., 2016; Berlioz et al., 2017). Dental microwear texture analysis informs on ecological niche partitioning and can also be used to highlight dietary differences between geographically (Bignon-Lau et al., 2017; Berlioz et al., 2022) and/or temporally distant populations (Berlioz et al., 2023). Dental microwear texture analysis is indeed a precious tool for characterizing the feeding ecology and trophic plasticity of fossil species (Scott et al., 2012; Berlioz et al., 2018) and making paleoenvironmental inferences (Merceron and Ungar, 2005; Merceron et al., 2007; Ungar et al., 2007). To interpret their feeding behavior, DMTA results from fossils are compared with those from modern populations whose environmental characteristics and diets are well known and cover the entire herbivore dietary spectrum (Table 1; Schubert et al., 2006; Merceron et al., 2007; Berlioz et al., 2023). In this study, we analyzed the occlusal enamel surface texture of 108 teeth of fossil *E. ferus*, seven *R. tarandus*, four *B. primigenius*/*Bi. priscus*, three *Megaloceros giganteus*, two *Coelodonta antiquitatis*, a *Cervus elaphus*, and a *Capra pyrenaica*, previously selected for the excellent preservation of their dental facets. We not only prioritized upper and lower second molars but also considered other molariform teeth, in accordance with the recommendations of Xafis et al. (2017) (SOM Table S1). The detailed molding and cleaning protocols are given here: https://doi.org/10.5281/zenodo.7305566. For all ungulates, except *C. antiquitatis*, the distolabial facet of the protoconid of lower molars or the mesiolingual facet of the protocone of upper molars was molded, following recommendations by Ramdarshan et al. (2017). For *C. antiquitatis*, following Hullot et al. (2019), we focused on the shearing facets of the lingual part of the protocone. Molding was performed at the TRACES Lab and the Centre Départemental d'Archéologie of Hasparren. Following the protocol detailed in Berlioz et al. (2023), molds were scanned using the Leica DCM8 white-light confocal profilometer TRIDENT at the PALEVOPRIM lab (UMR 7262) in Poitiers, France, using a 100× objective lens (numerical aperture = 0.90, working distance = 0.9 mm). We acquired a surface of 251 × 333 μm (2584 × 1945 cloud of points, z-step: 0.2 μm) at the center of the dental facet for each specimen. In cases where we identified major nondietary features on this surface (for more details and examples, see Weber et al., 2022; Micó et al., 2024a, 2024b), we slightly moved in order to acquire an area without taphonomic alterations.

Table 1
Reference populations used to interpret dental microwear texture analysis.

Dietary category	Species	*N*	References	Pop.
Grazer	*Cervus elaphus*	24	Berlioz (2017), Merceron et al. (2021)	1
	Bos taurus	43	Hermier et al. (2020)	2
	Equus quagga burchelli	20	Orlandi-Oliveras et al. (2022)	3
	Rangifer tarandus	52	Berlioz (2017), Bignon-Lau et al. (2017)	4
Mixed-feeder	*Cervus elaphus*	29	Berlioz (2017)	5
	Bison bonasus	19	Merceron et al. (2014)	6
	Rangifer tarandus	68	Berlioz (2017), Bignon-Lau et al. (2017)	7
Browser	*Cervus elaphus*	23	Berlioz (2017), Merceron et al. (2014)	8
	Equus africanus asinus	8	Orlandi-Oliveras et al. (2022)	9

Pop.: in the rest of the article, populations are referred to by their number.
Populations are classified by their dietary category (grazer, browser, or mixed-feeder).

In cases where this was not sufficient, the specimen was discarded. In total, 37.9% of dental surface molds were rejected at this stage due to the presence of exogenous elements on too large an area of the dental facet, excessive enamel damage, or bubbles formed during molding. We then sampled a 200 × 200-μm subsurface that we leveled and mirrored in Z. The few nonmeasured points (<3%) were replaced with a smooth shape using an algorithm calculated from neighboring points (nonmeasured points after cleaning: 0%). We applied the macro developed by Merceron et al. (2016) to remove abnormal peaks. Smaller artifacts and exogenous particles still present at this stage were manually removed and replaced by a smooth shape before a final leveling of the surface. In this way, they had no impact on the analysis. We finally removed a second-order least squares polynomial surface (PS2; Francisco et al., 2018a, 2018b) before extracting the DMTA-scale sensitive fractal analysis parameters at the EvoAdapta Lab with the LeicaMap software 9.3.10281 (SOM SI: 3–5; SOM Table S5). Area-scale fractal complexity (Asfc; hereafter 'complexity') quantifies surface roughness (Scott et al., 2009; Scott, 2012; DeSantis, 2016). Exact proportion of the length-scale anisotropy of the relief (epLsar; hereafter anisotropy) is used to quantify the preferential orientation of scars, mainly scratches, on enamel surfaces (Scott et al., 2006; Scott, 2012; DeSantis, 2016). Heterogeneity of the area-scale fractal complexity (HAsfc; hereafter heterogeneity) at 36 cells, calculated on each surface divided into 6 × 6 subsurfaces, describes the variations in complexity on a surface (Scott et al., 2006, 2009; DeSantis, 2016). Dental textures of browsers, which consume tougher lignified plants, poorer in abrasive silica and generally more brittle, are characterized by a lower epLsar than grazers, associated with a medium to high Asfc (Scott et al., 2005; Scott, 2012; Schulz et al., 2013; DeSantis, 2016). Heterogeneity, which reflects the diversity of food ingested, is also higher in browsers (Schulz et al., 2013). In supplementary information, we provide raw scans (.plux files; SOM SI: 4), photosimulations, and false color elevation maps (SOM SI: 5).

We conducted data exploration and statistics following Zuur et al. (2010) using RStudio v. 2023.03.1 Build 446 and the packages 'Hmisc,' 'corrplot,' 'onewaytests,' 'ggpubr,' 'ggplot2,' and 'magrittr.' Data were rank-transformed (Conover and Iman, 1981; Merceron et al., 2010) before conducting analyses of variance. When the initial conditions for parametric tests were not fulfilled, we carried out Kruskal-Wallis tests followed by Dunn's post hoc tests, whenever statistical differences were identified. We provide the R Markdown file in SOM 2. We compared the results of Isturitz ungulates from the three archaeostratigraphic units to DMTA parameter values obtained from nine extant reference populations belonging to six species, used as a comparative dataset (Table 1). These populations represent a continuum between a browsing and a grazing diet (Merceron et al., 2014, 2021; Berlioz, 2017; Bignon-Lau et al., 2017; Hermier et al., 2020; Berlioz et al., 2022; Orlandi-Oliveras et al., 2022). Then, we tested dietary differences among Isturitz equids through time. For the archaeostratigraphic unit Early Aurignacian, we also explored interspecific differences between contemporaneous equids and reindeer. When sample sizes were small (<5), we have not carried out statistical tests (for other fossil ungulates and units).

3. Results

3.1. Bayesian chronological model results

We have estimated the duration of the four different phases of human occupation based on the modeled calibrated dates (Rasmussen et al., 2014; Barshay-Szmidt et al., 2018; Reimer et al., 2020) (Fig. 2). A partial overlap is observed among phases, and phase 3 (layer C 4b2, corresponding to the Early Aurignacian, in Barshay-Szmidt et al., 2018) represents the longest duration. All phases are synchronous with MIS3 interstadials and stadials identified within the $\delta^{18}O$ record ice core from North Greenland Ice Core Project (SOM Table S6; SOM SI: 1). Phase 1 (Proto-Aurignacian; layer C 4d1 in Barshay-Szmidt et al., 2018) coincides with the end of Greenland Interstadial 11 and Greenland Stadial 11 (GS11) between 42,470 and 41,460 years cal BP, while phase 2 (Intermediate Aurignacian; layer C 4c4 in Barshay-Szmidt et al., 2018) is synchronous with the GS11 and part of the Greenland Interstadial 10 between 42,090 and 40,790 cal BP. Phase 3 corresponds to the first part of the Early Aurignacian (layer C 4b2 in Barshay-Szmidt et al., 2018) and is synchronous with the end of

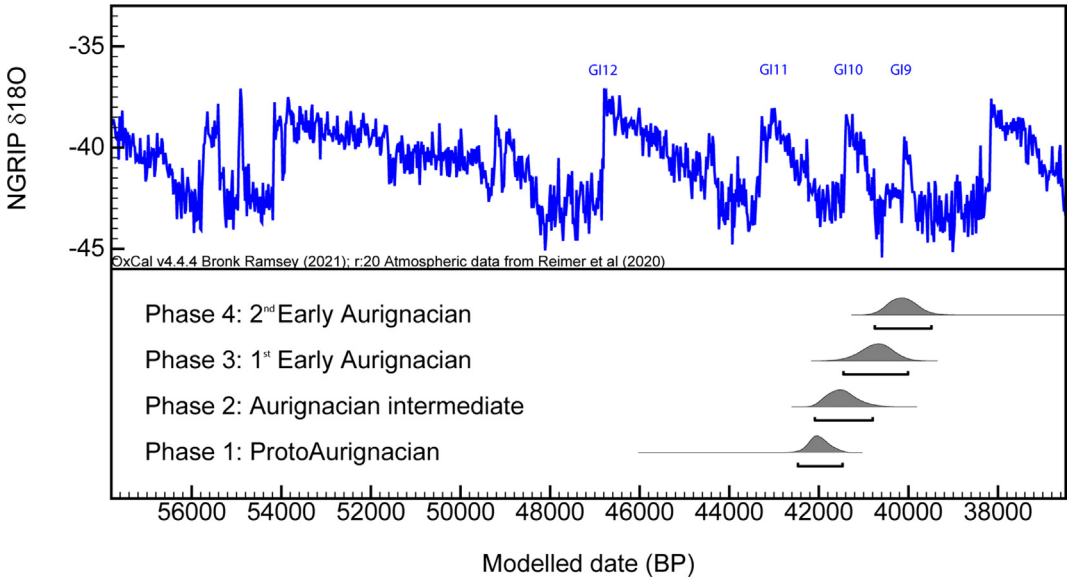

Figure 2. Radiocarbon-based chronology for Isturitz modeled using OxCal v.4.4.2 and the radiocarbon calibration curves IntCal20 (Reimer et al., 2020). Ultrafiltered radiocarbon dates from Barshay-Szmidt et al. (2018). Heinrich Stadial 4 (HS4) is shaded in blue, as per Sánchez Goñi and Harrison (2010). Greenland Interstadial (GI) onset ages are taken from Rasmussen et al. (2014). The sequence of posterior distributions summarizes the chronology of Aurignacian phases. NGRIP: North Greenland Ice Core Project. (For interpretation of the references to color in this figure legend, the reader is referred to the Web version of this article.)

Greenland Interstadial 10 and complete Greenland Stadial 10, between 41,450 and 40,000 cal BP. Phase 4, which belongs to the second part of the Early Aurignacian (layer C 4b1 in Barshay-Szmidt et al., 2018), is concomitant with Greenland Stadial 10, Greenland Interstadial 9, and Greenland Stadial 9, between 40,760 and 39,480 cal BP.

3.2. Enamel carbon and oxygen isotope data

Individual mean values for $\delta^{13}C_{carb}$ in horse teeth range from −11.6‰ to −11.2‰ for the Proto-Aurignacian ($N = 5$), from −10.4‰ to −10.1‰ for the Intermediate Aurignacian ($N = 2$), and from −10.9‰ to −9.9‰ for the Early Aurignacian ($N = 4$; Table 2). Subsequently, the estimated means on $\delta^{13}C_{diet}$ are lower during the Proto-Aurignacian (from −25.3‰ to −24.9‰) than during the Intermediate Aurignacian (from −24.1‰ to −23.8‰) and the Early Aurignacian (from −24.6‰ to −23.6‰) (Table 2, Fig. 3). The intratooth $\delta^{13}C_{carb}$ values reflect a range of variations from 0.5‰ to 1.7‰, with a mean range per archaeostratigraphic unit of 0.8‰ for the Proto-Aurignacian, 1.2‰ for the Intermediate Aurignacian, and of 1.1‰ for Early Aurignacian (Table 2).

Individual annual mean values for $\delta^{18}O_{carb}$ in horse teeth range from −6.5‰ to −5.7‰ for the Proto-Aurignacian ($N = 5$), are equal to −7.5‰ for the Intermediate Aurignacian ($N = 2$), and range from −6.9‰ to −6.1‰ for the Early Aurignacian ($N = 4$; Table 2). The resulting estimated mean $\delta^{18}O_{mw}$ value ranges from −9.2‰ to −7.9‰ during the Proto-Aurignacian and from −9.5‰ to −8.3‰ during the Early Aurignacian. Intermediate Aurignacian values are more negative, corresponding to −10.2‰.

Individual oxygen isotope curves demonstrate a sinusoidal intratooth pattern, with a range of intratooth $\delta^{18}O_{carb}$ values varying between 1.2‰ and 2.1‰ (Proto-Aurignacian = 1.9‰; Intermediate Aurignacian = 1.9‰; and Early Aurignacian = 1.5‰). There is a significant correlation between $\delta^{18}O_{carb}$ and $\delta^{13}C_{carb}$ ($p < 0.05$ in all cases), with a positive correlation for eight over 11 teeth. In all instances, r^2 values are low (0.05–0.51).

Mean annual temperature (Table 4) estimations based on $\delta^{18}O_{carb}$ values range from 6.7 °C to 11.1 °C, with a MAT of 10.6 ± 1 °C for the Proto-Aurignacian, 6.8 ± 0.1 °C for the Intermediate Aurignacian, and 9.5 ± 1.2 °C for the Early Aurignacian (Table 4 and SOM Table S4; SOM 6). In comparison, the present-day MAT at Isturitz (WorldClim) is 13.6 °C.

Mean annual precipitation (SOM Table S4) estimations based on $\delta^{13}C_{carb}$ values fluctuate between 214 and 445 mm (Tables 4 and SOM S4; SOM 6), higher for the Proto-Aurignacian (425 ± 25 mm) than for the more recent periods (258 ± 22 mm for the Intermediate Aurignacian and 280 ± 59 mm for the Early Aurignacian). In comparison, the current MAP at Isturitz equals 1229 mm.

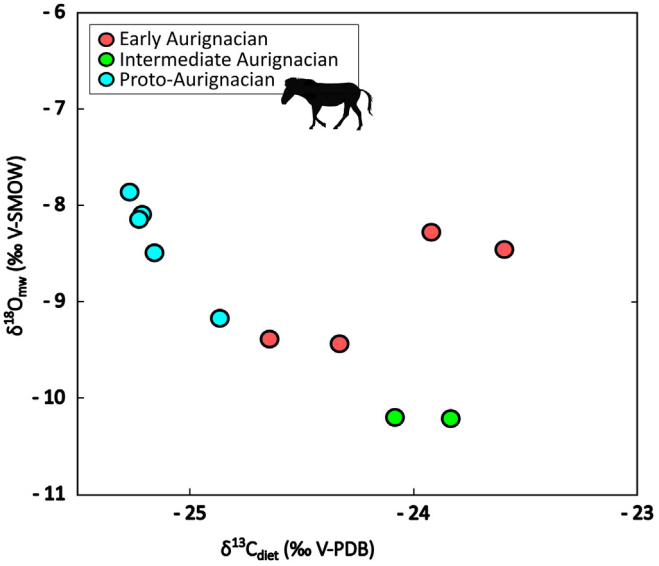

Figure 3. Bivariate plot representing individual $\delta^{13}C_{diet}$ and $\delta^{18}O_{mw}$ values from the tooth enamel of horses. V-PDB: Vienna Pee Dee Belemnite; V-SMOW: Vienna Standard Mean Ocean Water. (For interpretation of the references to color in this figure, the reader is referred to the Web version of this article.)

3.3. Bone collagen carbon, nitrogen, and sulfur isotope data

$\delta^{13}C$, $\delta^{15}N$, and $\delta^{34}S$ results are shown in Table 3 and in Figures 3 and 4. In Figure 4, $\delta^{13}C$ and $\delta^{15}N$ values are visually lower during the Proto-Aurignacian than during the Intermediate and Early Aurignacian. $\delta^{13}C$ values range between −21.7‰ and −18.6‰, and $\delta^{15}N$ values range between 4.2‰ and 13.3‰ (Fig. 4, Table 3, SOM Table S2).

Among ungulates, $\delta^{13}C$ values vary between −21.7‰ and −18.6‰ and $\delta^{15}N$ values between 4.2‰ and 13.3‰ (SOM Table S2). Bovines have a mean $\delta^{13}C$ value (±SD) of −20.6 ± 0.5‰ and a mean $\delta^{15}N$ value of 7.4 ± 1.9‰ (Table 3). Statistical analyses showed significant differences in $\delta^{13}C$ and $\delta^{15}N$ values between *B. primigenius*/*Bi. priscus* from the Proto-Aurignacian and the two more recent

Table 2
Stable isotope data ($\delta^{13}C$ and $\delta^{18}O$) extracted from tooth enamel of horses.

Code	Period	$\delta^{18}O_{carb}$ (‰ VPDB)							$\delta^{13}C_{carb}$ (‰ VPDB)					
		Annual mean	Mean	SD	Min.	Max.	Range	$\delta^{18}O_{mw}$	Mean	SD	Min.	Max.	Range	$\delta^{13}C_{diet}$
IST56	Early Aurignacian	**−6.8**	**−6.9**	0.4	−7.4	−6.2	1.2	−9.4	**−10.9**	0.3	−11.4	−10.6	0.8	−24.6
IST59		**−6.0**	**−6.1**	0.4	−7.2	−5.4	1.8	−8.3	**−10.2**	0.2	−10.6	−9.7	0.9	−23.9
IST61		**−6.1**	**−6.2**	0.4	−7.0	−5.3	1.6	−8.5	**−9.9**	0.3	−10.4	−9.5	0.9	−23.6
IST62		**−6.9**	**−6.9**	0.4	−7.4	−6.0	1.3	−9.5	**−10.6**	0.6	−11.4	−9.8	1.7	−24.3
IST121	Intermediate Aurignacian	**−7.5**	**−7.5**	0.6	−8.8	−6.7	2.1	−10.2	**−10.4**	0.3	−11.1	−9.7	1.4	−24.1
IST122		**−7.5**	**−7.5**	0.5	−8.3	−6.6	1.7	−10.2	**−10.1**	0.3	−10.7	−9.6	1.1	−23.8
IST95	Proto-Aurignacian	**−6.7**	**−6.5**	0.5	−7.1	−5.5	1.6	−9.2	**−11.2**	0.2	−11.4	−10.9	0.5	−24.9
IST96		**−6.2**	**−6.3**	0.5	−7.2	−5.2	2.0	−8.5	**−11.5**	0.2	−11.8	−11.2	0.6	−25.2
IST97		**−5.9**	**−6.0**	0.5	−6.8	−5.1	1.7	−8.1	**−11.5**	0.3	−11.9	−10.6	1.3	−25.2
IST98		**−5.7**	**−5.7**	0.5	−6.4	−4.6	1.8	−7.9	**−11.6**	0.2	−11.9	−11.3	0.6	−25.3
IST99		**−5.9**	**−5.8**	0.5	−7.0	−4.9	2.1	−8.2	**−11.5**	0.2	−12.0	−11.0	1.0	−25.2

Abbreviations: Min. = minimum value; Max. = maximal value; Range = max−min. Mean values are in bold.
All measurements are expressed relative to Vienna Pee Dee Belemnite (VPDB) notation, except for $\delta^{18}O_{mw}$ expressed in relation to Vienna Standard Mean Ocean Water (VSMOW). (Details of $\delta^{18}O_{mw}$ calculation are given in SOM S6.) The 'Annual mean' of $\delta^{18}O$ is obtained by averaging summer and winter from unmodeled isotope curves (except for IST62, ITS98, and IST121, where complete annual curves were not identified).

Table 3
Results of the bone collagen $\delta^{13}C$, $\delta^{15}N$, and $\delta^{34}S$ isotopic data for Isturitz herbivores and carnivores.

Species	Aurignacian	$\delta^{13}C$ V-PDB (‰)						$\delta^{15}N$ AIR (‰)						$\delta^{34}S$ V-CDT (‰)					
		N	Min.	Max.	Range	Mean	SD	*N*	Min.	Max.	Range	Mean	SD	*N*	Min.	Max.	Range	Mean	SD
Bovines	All	18	−21.6	−20.0	1.7	**−20.6**	**0.5**	18	4.2	10.4	6.3	**7.4**	**1.9**	19	11.2	15.5	4.3	**13.2**	**1.2**
	Early	5	−20.4	−20.0	0.3	**−20.3**	**0.3**	5	6.8	9.3	2.6	**9.2**	**1.4**	5	12.1	13.8	1.7	**13.0**	**1.5**
	Intermediate	7	−20.6	−20.0	0.7	**−20.2**	**0.1**	7	7.2	10.4	3.3	**7.9**	**0.9**	7	11.2	15.3	4.2	**12.9**	**0.6**
	Proto-	6	−21.6	−20.6	1.0	**−21.2**	**0.4**	6	4.2	6.4	2.2	**5.3**	**1.0**	7	12.2	15.5	3.3	**13.7**	**1.3**
Equus ferus	All	13	−21.7	−20.2	1.5	**−21.1**	**0.5**	13	4.3	10.3	6.0	**6.1**	**2.1**	11	10.0	15.4	5.4	**13.2**	**1.5**
	Early	4	−21.2	−21.1	0.1	**−20.7**	**0.6**	4	5.4	8.2	2.8	**8.2**	**2.3**	3	12.0	12.1	0.1	**12.6**	**2.4**
	Intermediate	2	−21.5	−20.2	1.3	**−21.1**	**0.0**	2	4.9	10.3	5.5	**6.8**	**2.0**	2	10.0	14.6	4.6	**12.0**	**0.1**
	Proto-	7	−21.7	−20.7	1.0	**−21.3**	**0.3**	7	4.3	6.1	1.8	**4.7**	**0.6**	6	12.7	15.4	2.7	**13.9**	**1.0**
Rangifer tarandus	All	8	−21.3	−18.6	2.7	**−19.7**	**0.9**	8	4.2	8.9	4.6	**7.6**	**1.6**	9	10.2	13.2	3.0	**11.9**	**1.1**
	Early	3	−19.2	−18.6	0.6	**−19.5**	**0.1**	3	8.2	8.7	0.5	**8.2**	**0.8**	3	10.7	13.2	2.6	**11.8**	**1.4**
	Intermediate	3	−19.7	−19.4	0.3	**−19.0**	**0.3**	3	7.3	8.9	1.6	**8.5**	**0.3**	4	10.2	12.6	2.4	**11.5**	**1.2**
	Proto-	2	−21.3	−21.1	0.2	**−21.2**	**0.1**	2	4.2	6.1	1.9	**5.2**	**1.3**	2	12.7	12.9	0.2	**12.8**	**0.1**
Cervus elaphus	All	3	−20.6	−20.4	0.3	**−20.5**	**0.1**	3	5.6	6.8	1.2	**6.1**	**0.6**	2	13.9	15.1	1.2	**14.5**	**0.8**
	Early																		
	Intermediate																		
	Proto-	3	−20.6	−20.4	0.3	**−20.5**	**0.1**	3	5.6	6.8	1.2	**6.1**	**0.6**	2	13.9	15.1	1.2	**14.5**	**0.8**
Vulpes sp.	All	6	−20.3	−19.4	0.9	**−19.9**	**0.4**	6	7.1	13.3	6.2	**9.3**	**2.3**	6	1.6	15.1	13.5	**11.0**	**4.7**
	Early	2	−20.3	−19.5	0.8	**−19.9**	**0.1**	2	7.1	10.1	3.0	**11.5**	**2.5**	2	11.7	12.6	0.8	**12.1**	**0.6**
	Intermediate	2	−20.0	−19.9	0.1	**−19.9**	**0.6**	2	9.7	13.3	3.6	**8.6**	**2.1**	2	1.6	13.0	11.4	**7.3**	**8.1**
	Proto-	2	−20.2	−19.4	0.8	**−19.8**	**0.6**	2	7.6	7.9	0.3	**7.8**	**0.2**	2	12.0	15.1	3.1	**13.5**	**2.2**
Ursus sp.	All	1				**−19.3**		1				**10.9**		1				**12.3**	
	Early																		
	Intermediate																		
	Proto-	1				−19.3		1				−19.3		1				−19.3	

Abbreviations: Min. = minimum value; Max. = maximal value; Range = range of variation. Mean and standard deviation (SD) are in bold.

archaeostratigraphic units (*p* values of, respectively, 0.015 and 0.01; SOM 2), with lower values during the Proto-Aurignacian ($\delta^{13}C_{Proto.}$ = −21.2 ± 0.4‰ and $\delta^{15}N_{Proto.}$ = 5.3 ± 0.9‰; SOM Table S2). Although not statistically tested ($N < 5$), the same trend is observed, with an even greater increase in mean $\delta^{13}C$ values for *R. tarandus* ($\delta^{13}C_{Proto.}$ = −21.2 ± 0.1‰, $\delta^{13}C_{Intermed.}$ = −19.0 ± 0.3‰, and $\delta^{13}C_{Early}$ = −19.5 ± 0.1‰; and $\delta^{15}N_{Proto.}$ = 5.2 ± 1.3‰, $\delta^{15}N_{Intermed.}$ = 8.4 ± 0.3‰, and $\delta^{15}N_{Early}$ = 8.2 ± 0.8‰; Table 3). In *E. ferus*, an increase in $\delta^{15}N$ values over time is observed, associated with an increase in interindividual variability between the Proto-Aurignacian and the Intermediate and Early Aurignacian ($\delta^{15}N_{Proto.}$ = 4.7 ± 0.6‰, $\delta^{15}N_{Intermed.}$ = 6.8 ± 2.0‰, and $\delta^{15}N_{Early}$ = 8.2 ± 2.3‰; Table 3), while $\delta^{13}C$ values remain little changed through time ($\delta^{13}C_{Proto.}$ = −21.3 ± 0.3‰, $\delta^{13}C_{Intermed.}$ = −21.1 ± 0.0‰, and $\delta^{13}C_{Early}$ = −20.7 ± 0.6‰).

Statistical tests performed revealed no significant difference in $\delta^{13}C$ (p = 0.71; SOM 2) and $\delta^{15}N$ (p = 0.26, SOM 2) between contemporaneous Proto-Aurignacian *E. ferus* (N = 7) and *B. primigenius*/*Bi. priscus* (N = 6). The three Proto-Aurignacian *Ce. elaphus* have higher $\delta^{15}N$ and less negative $\delta^{13}C$ values than other contemporary ungulates ($\delta^{13}C_{Proto.}$ = −20.5 ± 0.1‰, $\delta^{15}N_{Proto.}$ = 6.1 ± 0.6‰; SOM Table S2).

Among carnivores, the single *Ursus* sp. individual has a $\delta^{13}C_{Proto.}$ = −19.3‰ and the $\delta^{15}N_{Proto.}$ value is high (10.9‰; Table 3). Due to these high $\delta^{15}N$ values and the fragmentation state of this third phalanx, zooarchaeology by mass spectrometry analysis confirmed its taxonomy, corroborating its archaeozoological identification.

The $\delta^{13}C$ values of *Vulpes* sp. change little over time (Table 3), with greater interindividual variability during the Proto-Aurignacian and Intermediate Aurignacian ($\delta^{13}C_{Proto.}$ = −19.8 ± 0.6‰, $\delta^{13}C_{Intermed.}$ = −19.9 ± 0.6‰, and $\delta^{13}C_{Early}$ = −19.9 ± 0.1‰). As for $\delta^{15}N$, values increase at the Early Aurignacian, with greater interindividual differences at the Intermediate and Early Aurignacians ($\delta^{15}N_{Proto.}$ = 7.8 ± 0.2‰, $\delta^{15}N_{Intermed.}$ = 8.6 ± 2.1‰, and $\delta^{15}N_{Early}$ = 11.5 ± 2.5‰; Table 3).

$\delta^{34}S$ values for Isturitz macrofauna range between 1.6‰ and 15.4‰ (SOM Table S2). They are particularly high for ungulates, ranging between 10.0‰ and 15.4‰ (Fig. 5), while there is more interindividual variability among carnivores (values between 1.6‰ and 15.1‰; Fig. 5, SOM Table S2). For *B. primigenius*/*Bi. priscus* (≥5 in each unit), no significant differences were found between the three archaeostratigraphic units (p = 0.49; $\delta^{34}S_{Proto.}$ = 13.7 ± 1.3‰, $\delta^{34}S_{Intermed.}$ = 12.9 ± 0.6‰, and $\delta^{34}S_{Early}$ = 13.0 ± 1.5‰; Table 3; SOM 2). Horses and reindeer show similar values (mean $\delta^{34}S_{Equus}$ = 13.2 ± 1.5‰; mean $\delta^{34}S_{Rangifer}$ = 11.9 ± 1.1‰) and the same stability over time. The two Proto-Aurignacian *Ce. elaphus* also have high $\delta^{34}S$ values (mean $\delta^{34}S$ = 14.5 ± 0.8‰; Table 3).

Statistical tests revealed no significant difference in $\delta^{34}S$ between Proto-Aurignacian bovids and equids (p = 0.9; SOM 2).

Regarding carnivores, the only bear specimen (*Ursus* sp.) is not differentiated by its $\delta^{34}S$ value ($\delta^{34}S$ = 12.3‰; Table 3). If we except one outlier specimen from the intermediate Aurignacian ($\delta^{34}S_{outlier}$ = 1.6‰; SOM Table S2, Fig. 5), *Vulpes* sp. remains in the same range of values throughout the sequence (mean $\delta^{34}S$ = 12.9 ± 0.6‰).

Table 4
Climatic estimations based on stable isotope composition ($\delta^{13}C$ and $\delta^{18}O$) of horse teeth.[a]

Period	*N*	Past climatic estimations		Difference to present	
		MAT (°C)	MAP (mm)	MAT (°C)	MAP (mm)
Early Aurignacian	4	9.5	280 ± 59	−4.1	−948
Intermediate Aurignacian	2	6.8	258 ± 22	−6.8	−971
Proto-Aurignacian	5	10.6	425 ± 25	−3.0	−804

Details of calculations and errors are explained in SOM S6.
Abbreviations: MAT = mean annual temperature; MAP = mean annual precipitation.
[a] Current climatic data (MAT = 13.6 °C; MAP = 125 mm) extracted from WorldClim dataset v2.

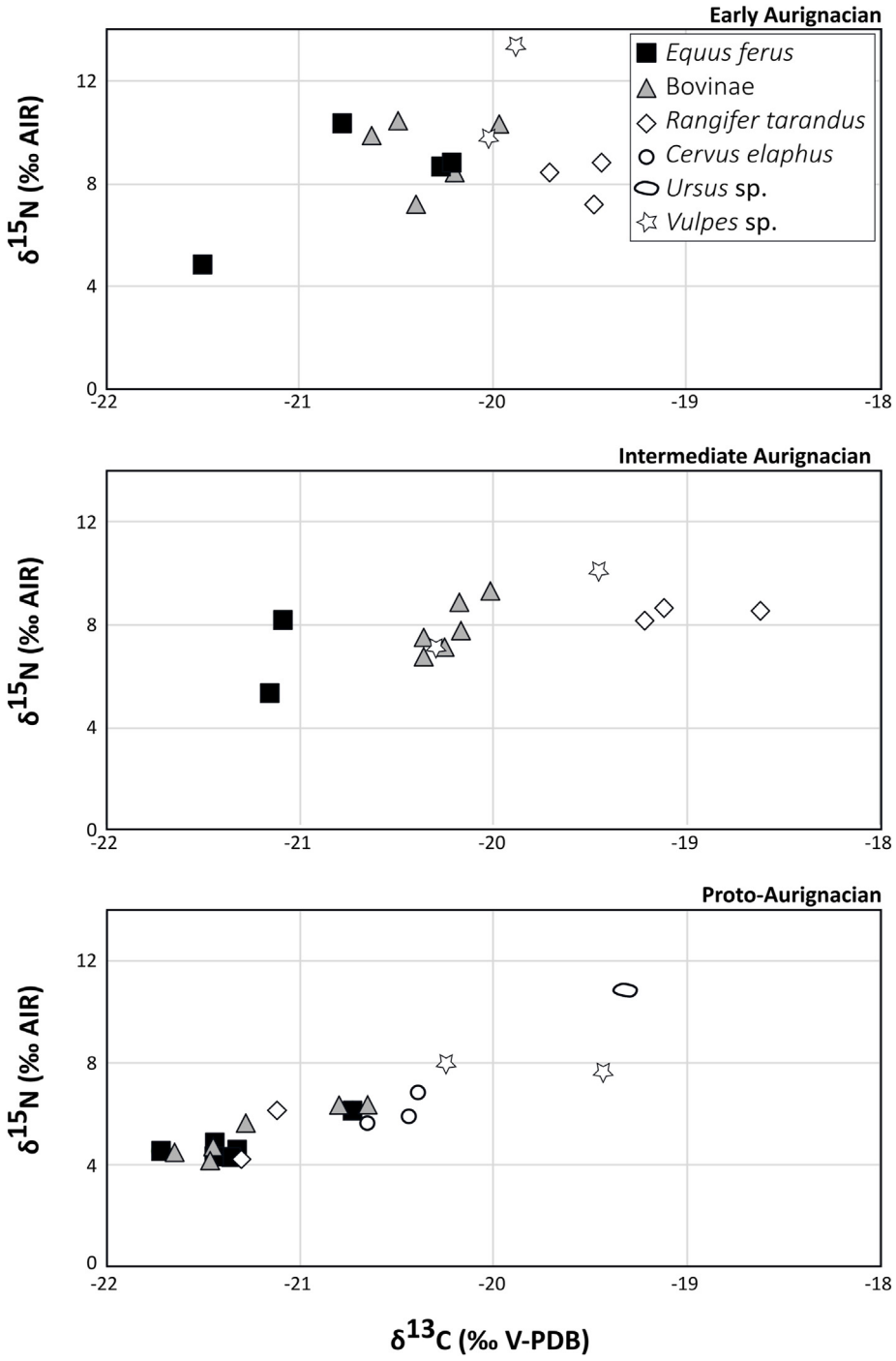

Figure 4. $\delta^{13}C$ and $\delta^{15}N$ values from the bone collagen of Isturitz ungulates and carnivores from the Proto-Aurignacian, Intermediate Aurignacian, and Early Aurignacian. V-PDB: Vienna Pee Dee Belemnite; AIR: atmospheric air.

3.4. Three-dimensional dental microwear texture analysis

Nine modern populations as an interpretative framework The four populations of modern herbivores representing the grazer category (populations 1, 2, 3, and 4: Table 1, the lower part of Table 5, Fig. 6) are characterized by low complexities (Asfc < 2.00) and low to medium heterogeneities of the complexity (HAsfc < 0.700), coupled with high anisotropies (epLsar > 4.00). The two browser populations (populations 8 and 9: Table 1, the lower part of Table 5, Fig. 6) show values typical of this dietary category, with low anisotropies (epLsar < 4.00) coupled with high complexities (Asfc > 2.00) and intermediate to high heterogeneities of the complexity (HAsfc > 0.600). Finally, mixed-feeders, represented here by three modern populations (populations 5–7: Table 1, the lower part of Table 5, Fig. 6), are characterized by intermediate values of their texture parameters.

Fossil distribution Results for fossils are discussed based on the herbivore dietary spectrum defined based on the nine extant

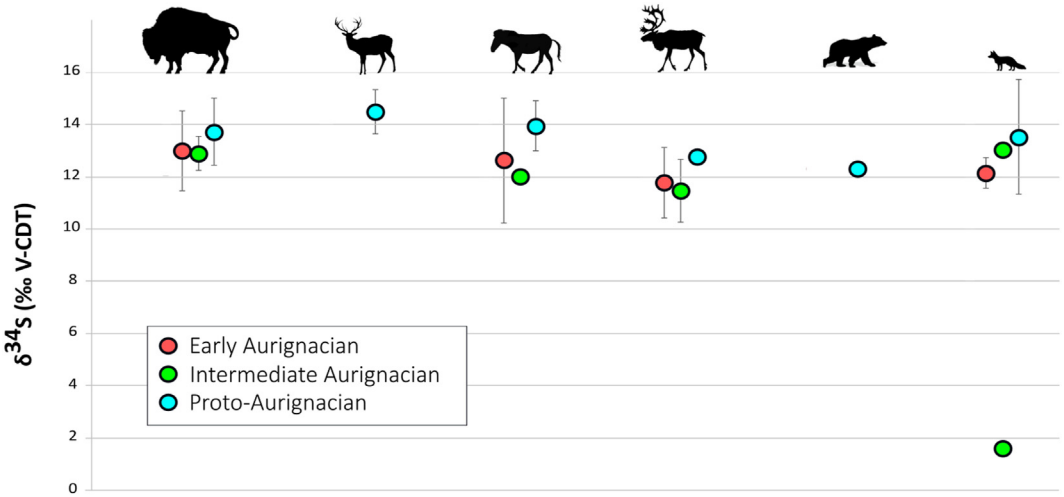

Figure 5. $\delta^{34}S$ values from the bone collagen of Isturitz ungulates and carnivores. Mean values (for $N \geq 2$) associated with SD are given for the three archaeostratigraphic units. V-CDT: Vienna-Canyon Diablo Troilite. For Intermediate Aurignacian foxes, individual data are provided, allowing us to identify a specimen with an exceptionally low $\delta^{34}S$ value. (For interpretation of the references to color in this figure, the reader is referred to the Web version of this article.)

Table 5
Results of the DMTA-SSFA of Isturitz ungulates.

Species	Aurignacian	*N*	Asfc				epLsar (10^{-3})				HAsfc			
			Mean	SD	SEM	95% CI	Mean	SD	SEM	95% CI	Mean	SD	SEM	95% CI
Coelodonta antiquitatis	All	**2**	**1.67**	1.26	0.89	1.78	**2.18**	0.91	0.64	1.28	**0.374**	0.015	0.010	0.021
	Early	0												
	Intermediate	0												
	Proto-	**2**	**1.67**	1.26	0.89	1.78	**2.18**	0.91	0.64	1.28	**0.374**	0.015	0.010	0.021
Bovines	All	**4**	**1.69**	1.05	0.53	1.05	**4.60**	4.09	2.05	4.09	**0.396**	0.053	0.026	0.053
	Early	1	**1.44**				**5.36**				**0.405**			
	Intermediate	1	**3.22**				**0.62**				**0.464**			
	Proto-	2	**1.05**	0.32	0.23	0.45	**6.22**	5.36	3.79	7.57	**0.358**	0.028	0.020	0.040
Equus ferus	All	**108**	**1.54**	0.67	0.06	0.13	**4.25**	1.91	0.18	0.37	**0.430**	0.144	0.014	0.028
	Early	45	**1.65**	0.76	0.11	0.23	**3.99**	1.97	0.29	0.59	**0.432**	0.123	0.018	0.037
	Intermediate	9	**1.36**	0.53	0.18	0.35	**3.90**	1.86	0.62	1.24	**0.531**	0.151	0.050	0.101
	Proto-	54	**1.49**	0.61	0.08	0.17	**4.52**	1.86	0.25	0.51	**0.522**	0.169	0.023	0.046
Rangifer tarandus	All	**7**	**1.68**	0.70	0.26	0.53	**6.58**	0.85	0.32	0.64	**0.448**	0.194	0.073	0.147
	Early	6	**1.55**	0.67	0.27	0.55	**6.77**	0.76	0.31	0.62	**0.477**	0.195	0.080	0.159
	Intermediate	0												
	Proto-	1	**2.44**				**5.48**							
Megaloceros giganteus	All	**3**	**1.23**	0.35	0.20	0.40	**6.10**	1.51	0.87	1.74	**0.501**	0.116	0.067	0.134
	Early	3	**1.23**	0.35	0.20	0.40	**6.10**	1.51	0.87	1.74	**0.501**	0.116	0.067	0.134
	Intermediate	0												
	Proto-	0												
Cervus elaphus	All	**1**	**0.87**				**2.70**				**0.310**			
	Early	0												
	Intermediate	1	**0.87**				**2.70**				**0.310**			
	Proto-	0												
Capra pyrenaica	All	**1**	**1.67**				**7.14**				**0.411**			
	Early	1	**1.67**				**7.14**				**0.411**			
	Intermediate	0												
	Proto-	0												
Grazers	1	**24**	**1.24**	0.57	0.12	0.23	**6.11**	2.43	0.50	0.99	**0.630**	0.463	0.094	0.189
	2	**43**	**1.56**	0.92	0.14	0.28	**5.27**	2.11	0.32	0.64	**0.563**	0.274	0.042	0.083
	3	**20**	**1.73**	0.99	0.22	0.44	**5.98**	2.16	0.48	0.96	**0.493**	0.161	0.036	0.072
	4	**52**	**1.76**	0.64	0.09	0.18	**4.21**	2.03	0.28	0.56	**0.698**	0.300	0.042	0.083
Mixed-feeder	5	**29**	**2.13**	0.80	0.15	0.30	**4.29**	2.02	0.37	0.75	**0.651**	0.329	0.061	0.122
	6	**19**	**2.03**	1.11	0.25	0.51	**3.89**	2.11	0.48	0.97	**0.603**	0.376	0.086	0.173
	7	**68**	**2.30**	1.08	0.13	0.26	**3.15**	1.54	0.19	0.37	**0.769**	0.342	0.041	0.083
Browser	8	**23**	**2.82**	1.74	0.36	0.73	**3.11**	1.24	0.26	0.52	**0.674**	0.299	0.062	0.125
	9	**8**	**5.87**	5.97	2.11	4.22	**2.88**	1.60	0.57	1.13	**0.799**	0.369	0.131	0.261

Abbreviations: SEM = standard error of the mean; 95% CI = 95% confidence interval of the mean; DMTA-SSFA = dental microwear texture analysis – scale-sensitive fractal analysis; Asfc = area-scale fractal complexity; epLsar (10^{-3}) = exact proportion of the length-scale anisotropy of the relief; HAsfc = heterogeneity of the area-scale fractal complexity (6 × 6 cells). Mean values are in bold.

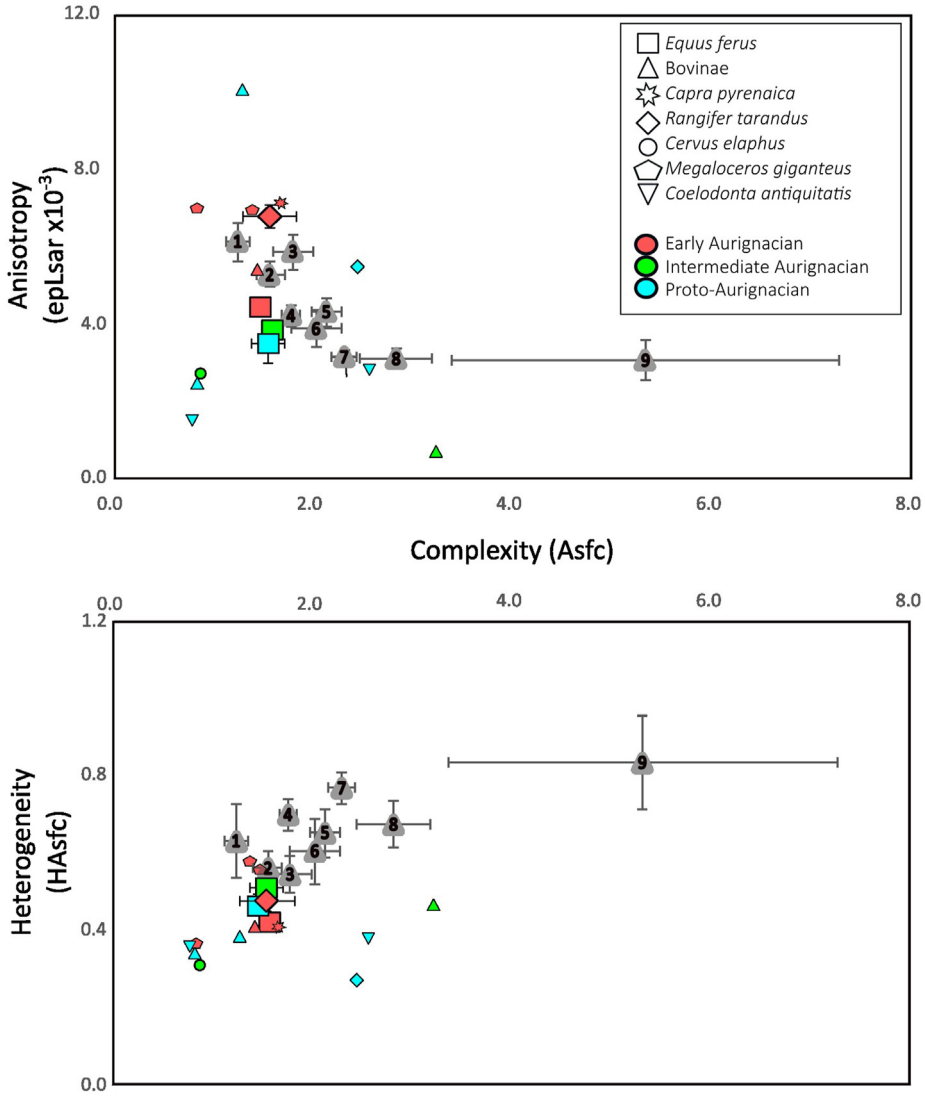

Figure 6. Bivariate plots representing three dental microwear texture analysis parameters. Upper part: complexity and anisotropy. Lower part: complexity and heterogeneity of the complexity. The three colors represent the three archaeostratigraphic units. Symbols are different for each species. Mean values associated with standard error of mean are given whenever $N \geq 5$. Otherwise, individuals are represented. Gray triangles refer to reference populations, corresponding to grazers (1: *Cervus elaphus*, Bauges, 2: *Bos taurus*, Camargue, 3: *Equus quagga burchelli*, and 4: *Rangifer tarandus*, Knutshø), mixed-feeders (5: *Ce. elaphus*, Chateauroux, 6: *Bison bonasus*, Białowieża, and 7: *R. tarandus*, Hardangervidda), and browsers (8: *Ce. elaphus*, Białowieża, 9: *Equus africanus asinus*). Asfc = area-scale fractal complexity; HAsfc = heterogeneity of the area-scale fractal complexity; epLsar = exact proportion of the length-scale anisotropy of the relief. (For interpretation of the references to color in this figure legend, the reader is referred to the Web version of this article.)

European herbivore populations with well-known diets described earlier. The only early Aurignacian specimen of *Ca. pyrenaica* displays a high anisotropy (epLsar = 7.14 × 10^{-3}; Table 5, SOM Table S5, Fig. 6) paired with low complexity (Asfc = 1.67) and heterogeneity of the complexity (HAsfc = 0.411). The results for the three *M. giganteus* from the same archaeostratigraphic unit are comparable (mean epLsar ± 95% confidence interval = 6.10 ± 1.74 × 10^{-3}; mean Asfc = 1.23 ± 0.40; mean HAsfc = 0.501 ± 0.134). Our sample includes four *B. primigenius*/*Bi. priscus*, with two Proto-Aurignacian individuals exhibiting high anisotropy (mean epLsar = 6.22 ± 7.57 × 10^{-3}), low complexity (mean Asfc = 1.05 ± 0.45), and low heterogeneity of the complexity (mean HAsfc = 0.358 ± 0.040; Table 5). The unique early Aurignacian bovine falls within this same range of values, whereas the specimen from the Intermediate Aurignacian displays markedly different values (low epLsar = 0.62 × 10^{-3}, high Asfc = 3.22, and low HAsfc = 0.464). The *Ce. elaphus* from the Intermediate Aurignacian is characterized by low anisotropy, complexity, and heterogeneity of the complexity (epLsar = 2.70 × 10^{-3}, Asfc = 0.87, and HAsfc = 0.310). Reindeer are characterized by an extensive range of values for complexity (mean Asfc = 1.68 ± 0.26). At the same time, anisotropy is high for all seven specimens (mean epLsar = 6.58 ± 0.64 × 10^{-3}), and heterogeneity of the complexity (HAsfc) is low for all but one specimen (SOM Table S5). The complexity of the two Proto-Aurignacian *C. antiquitatis* varies (mean Asfc = 1.67 ± 1.78), while they are characterized by low anisotropy (mean epLsar = 2.18 ± 1.28 × 10^{-3}) and heterogeneity of the complexity (mean HAsfc = 0.37 ± 0.02). The 108 *E. ferus* teeth display low

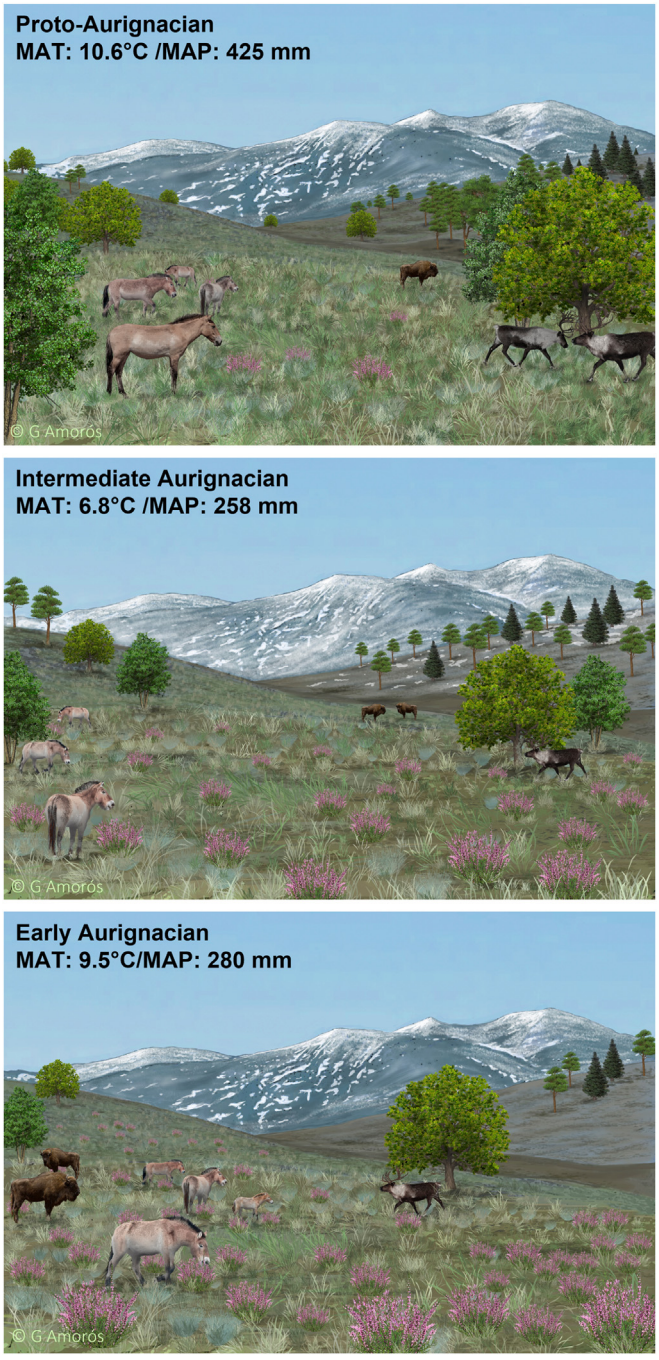

Figure 7. Paleoartistic representations of the environment surrounding the Isturitz cave during the different phases of Aurignacian human occupations, based on palynological analyses (Leroi-Gourhan, 1959; Normand et al., 2007; Fourcade et al., 2022) and the results of the present study. Author: Gabriela Amorós Seller. MAP = mean annual precipitation; MAT = mean annual temperature. (For interpretation of the references to color in this figure, the reader is referred to the Web version of this article.)

complexity (mean Asfc = 1.54 ± 0.13; Table 5) and heterogeneity (mean HAsfc = 0.430 ± 0.028), associated with high anisotropy (mean epLsar = 4.25 ± 0.37 × 10^{-3}). Dental microwear texture analysis values for equids are very similar between the three archaeostratigraphic units ($p > 0.05$; SOM 2). For the Early Aurignacian, the only difference between the horse and reindeer is their anisotropy ($p = 0.0039$; SOM 2), being higher for *R. tarandus* (6.77 ± 0.36 × 10^{-3} for reindeer vs. 3.99 ± 0.59 × 10^{-3} for horse; Table 5, SOM Table S4, Fig. 6).

4. Discussion

4.1. Chronological reassessment of the chronology of Isturitz's early occupations

The Bayesian modeling of available ^{14}C dates (Barshay-Szmidt et al., 2018) calibrated with the new IntCal20 curve developed in this work provides an updated temporality of the human occupation phases at Isturitz. It gives slightly older ages than those mentioned in Barshay-Szmidt et al. (2018), confirming that the abrupt HS4 climatic event could not have triggered the Early Aurignacian technological change, a hypothesis previously proposed by Banks et al. (2013) and Banks (2017).

4.2. Combining three ecological proxies for an in-depth reconstruction of the Isturitz local ecosystem

Climatic reconstruction As expected, based on $\delta^{18}O_{carb}$ measurements from tooth enamel, climatic reconstructions at Isturitz support temperatures colder than present-day for the Proto-Aurignacian ($MAT_{Proto.}$ = 10.6 °C and $MAT_{present\text{-}day}$ = 13.6 °C). Annual temperatures are even colder during Intermediate and Early Aurignacians ($MAT_{Intermed.}$ = 6.8 °C and MAT_{Early} = 9.5 °C; Fig. 7). Increasing $\delta^{15}N$ and $\delta^{13}C_{carb}$ values associated with slightly more negative $\delta^{18}O_{carb}$ values for more recent Aurignacian units than the Proto-Aurignacian suggest a simultaneous decrease in moisture through time (Fig. 4; Table 2). This is reflected in precipitation levels that decrease from the Proto-Aurignacian onward, representing notably lower values than present-day (between −971 mm and −804 mm). These results attest the Aurignacian human occupation at Isturitz occurred in a context of extreme cold, which then rapidly intensified throughout the sequence, coupled with drier local climatic conditions. The $\delta^{18}O_{carb}$ values of Isturitz horses, in particular the Intermediate Aurignacian values, are comparable to those observed at Labeko Koba, a contemporary cave site in the Cantabrian region (Fernández-García et al., 2024).

Our findings are corroborated by palynological analyses at the site, which also reflect a "*gradual cooling through time, albeit interspersed with at least a slight climatic improvement*" (Leroi-Gourhan, 1959; *fide* Normand et al., 2007, p. 7). It also coincides with what has been shown at the more regional scale of the Bay of Biscay study of the core MD04-2845 (Sánchez Goñi et al., 2008; Fourcade et al., 2022). During Isturitz Proto-Aurignacian, Atlantic forests and semidesert steppes are abundant in the region (Fourcade et al., 2022). During the Intermediate Aurignacian, the Atlantic Forest cover declines, replaced by boreal forests, and the semiarid steppe is rapidly replaced by heather, rich in *Calluna*. During the two phases of the Early Aurignacian, core pollen from the Bay of Biscay indicates open paleoenvironments with low forest cover associated with heather (including *Calluna*), accounting for an even more significant portion of the vegetation (Fourcade et al., 2022).

The Intermediate Aurignacian of Isturitz exhibits particularly low $\delta^{18}O_{carb}$ and high $\delta^{13}C_{carb}$ suggesting even colder and more arid conditions, perhaps coinciding with one of the coldest episodes of the GS11 (Fig. 2). The isotopic analysis was conducted at the local scale of human and ungulate territories of Isturitz, while the pollinic study that incorporates deposits from various sources of the French and Spanish Atlantic coasts, which are not exempt from problems regarding the origin of pollen spectra, provides a regional overview (Fourcade et al., 2022). Nevertheless, the local impact of global climate changes is also determined by habitat characteristics, including geology, topography, altitude, latitude, and distance from the ocean, which could explain why these local climate variations are not visible on a more regional scale.

Fauna mobility $\delta^{34}S$ values observed for ungulates preyed on by human groups (between 10.0‰ and 15.4‰ V-CDT; SOM Table S2) are in the higher range of values observed for other archaeological localities of the Franco-Iberian region (Jones et al., 2018; Britton et al., 2023; Pederzani et al., 2023). Several factors, including bedrock, soil type, and the impact of sea spray (Nehlich, 2015), could explain these high values, making a definitive explanation of the causes of such results difficult (Pederzani et al., 2023). But what is particularly interesting about these results is their remarkable stability over time and the homogeneity of values between the ungulate and carnivore species considered since this has substantial implications in terms of humans' choice of hunting territories over time (Jones et al., 2019). Indeed, these results suggest that, despite significant environmental changes induced by abrupt and continuous climatic oscillations between the Proto-Aurignacian and Early Aurignacian, human populations did not radically modify their hunting territories during this period, meaning that these territories continued to satisfy their needs sufficiently.

The role of Carnivora in the Isturitz food web Among Isturitz Carnivora, the only bear (*Ursus* sp.) analyzed presents $\delta^{34}S$ values similar to contemporaneous preyed ungulates (12‰ V-CDT; Table 3), arguing in favor of a territory akin to the hunting territory of human populations. The combination of its $\delta^{13}C_{coll}$ and high $\delta^{15}N$ values could suggest that this individual behaved as a large hypercarnivore (Bocherens, 2015), which would contrast with the highly plant-dependent diet known for European cave bears (Pacher and Stuart, 2009), associated with low $\delta^{15}N$ values. For their part, the brown bear has a more omnivorous diet (Bojarska and Selva, 2012), and many fossil specimens do not reach such high $\delta^{15}N$ values either (Bocherens et al., 2004; Bocherens, 2015). In addition, the $\delta^{15}N$ values of this specimen are at least >3% higher than those of sympatric herbivores. A recent study by Naito et al. (2020) highlighted the very high $\delta^{15}N$ values of some Romanian cave bears were due to the consumption of high-$\delta^{15}N$ plants, rather than the effect of the higher trophic level of meat consumption. Although this question would need to be explored for Isturitz bear, the interpretations of these authors nevertheless provide an interesting avenue for reflection on our results.

Foxes, representing most of the carnivores at the site (Soulier et al., 2014), remain in the same range of $\delta^{34}S$ values throughout the sequence (11.7–15.1‰ VCDT), except for the ulna of one fox that has a very low value (1.62‰ VCDT; Fig. 5) which could support a distinct geographical origin or be an outlier. The archaeozoological study (Soulier, 2013; table 2.4.8) reveals numerous signs of human exploitation on fox bones at Isturitz (see also Costamagno, 2017), with defleshing, disarticulation, and skinning marks during the Proto-Aurignacian and the Early Aurignacian levels. One explanation for this extreme value could be a human transport of this bone element from a fox captured in a different isotopic landscape. Among foxes, the $\delta^{13}C_{coll}$ and $\delta^{15}N$ values indicate an omnivorous diet typical of these species, with varying proportions of meat, berries, or fruit consumption among individuals.

Ungulate's ecological responses This common regional origin of the predated species throughout the sequence also allows us to establish with greater certainty the link between the ungulates' ecological responses and the climate's evolution at a local scale. Both the $\delta^{13}C_{coll}$ values of the ungulates and the $\delta^{13}C_{diet}$ values for equids (Tables 2 and 3), the most abundant species of the faunal assemblage, indicate the consumption of terrestrial C3 plants, as expected for this region at that time. All along the sequence, high values are incompatible with a 'canopy effect' (i.e., an extensive tree cover: Drucker et al., 2008; Bonafini et al., 2013). In parallel, $\delta^{13}C_{diet}$ and $\delta^{15}N$ align with what is expected of grazers (Drucker et al., 2008; Bocherens et al., 2015). We observe similar tendencies in bone collagen for all ungulate species, whether selective or ecologically plastic. The $\delta^{13}C_{carb}$ values of Isturitz equids are higher than in the contemporaneous levels of the site of Labeko-Koba located near Bilbao (Fernández-García et al., 2024) but similar to those from the north-eastern Spanish sites of Terrasses de la Riera dels Canyars (Gavà, Catalonia; Fernández-García et al., 2024) and Arbreda (Serinyà, Catalonia; Drucker et al., 2024), reflecting more open landscapes related to arid events.

Therefore, we interpret that these ungulates inhabited open landscapes and primarily grazed throughout their lives. Such results also reveal the ecological conditions in the surroundings of Isturitz under which Aurignacian humans lived.

Significant $\delta^{13}C_{coll}$ and $\delta^{15}N$ differences between Proto-Aurignacian bovines and the Intermediate and Early Aurignacian point to a shift toward even more open habitats from the Intermediate Aurignacian onward (Fig. 7). As mentioned earlier, 'Bovines' include representatives of both *B. primigenius* and *Bi. priscus* that are difficult to distinguish based on their dental morphology and are potentially different in terms of ecology. However, our results show few interindividual differences within each archaeostratigraphic unit (Fig. 4). Although this result was not tested statistically, the same trend in $\delta^{13}C_{coll}$ and $\delta^{15}N$ was found for reindeer and horses (Table 3). The $\delta^{13}C_{carb}$ measurements from horse teeth show concordant results (Table 2). Such results are compatible with the decrease in estimated MAP between the Proto-Aurignacian and Early Aurignacian (Table 4) and with the gradual opening of landscapes recorded on local (Leroi-Gourhan, 1959; Normand et al., 2007) and regional scales (Fourcade et al., 2022). This landscape opening has also been detected in archaeological sites of the North Atlantic Cantabrian region, using a combination of multiclimatic proxies (Fernández-García et al., 2023).

The difference in $\delta^{13}C_{coll}$ values between the Proto-Aurignacian and the Intermediate and Early Aurignacian is even more pronounced for reindeer (Table 3). Less negative $\delta^{13}C_{coll}$ values for reindeer than for coeval ungulates are often related to the diversity of plants eaten by this species. It has been shown that lichens, which can make up a very large proportion of reindeer diet whenever other resources are lacking (Geist, 1998), are enriched in ^{13}C (Drucker et al., 2001; Bocherens, 2015; Britton et al., 2023). This finding suggests that the regional cooling during the Intermediate and Early Aurignacian may have facilitated reindeer's access to ^{13}C-enriched resources and led to a shift in their feeding behavior. Such a result illustrates the opportunistic behavior of this species (Geist, 1998). These dietary changes coincide with increased reindeer abundance after the Proto-Aurignacian (Figs. 1 and 7), which could suggest the presence of individuals in environmental conditions more suited to their needs.

One horse specimen from the Intermediate Aurignacian presents a more negative $\delta^{13}C_{coll}$ value associated with a $\delta^{34}S$ value similar to other specimens, indicating a greater reliance on forested habitats throughout its life rather than a different geographical origin (Table 3). Proto-Aurignacian red deer, represented by only three individuals, shows less negative $\delta^{13}C_{coll}$ values than other ungulates in the same archaeostratigraphic unit. Such a result may reflect the niche partitioning between sympatric ungulates, with red deer occupying more open habitats and/or consuming more graze.

Unlike the other proxies of this study, DMTA reflects the last few days or weeks of the life of an animal (Teaford and Glander, 1991; Merceron et al., 2010; Winkler et al., 2020), which, in the case of hunted animals, corresponds to the vegetation they have been eating during the hunting season (Table 5). Dental microwear texture analysis indicates a grazing diet for *E. ferus*, the main species present throughout the sequence, meaning that these animals consumed a considerable amount of herbaceous monocotyledons shortly before their death. These results are congruent with those obtained from their $\delta^{13}C_{coll}$ measurements (Table 3), which provides us with information on the average diet of these animals

throughout their lives, and those obtained from the $\delta^{13}C_{diet}$ in the enamel of their third molars (Table 2), which documents the diet between the second and fifth years of their life (Hoppe et al., 2004). The other ungulates of the site, whether selective or ecologically plastics, although not numerous enough to have been statistically analyzed, support the same trend of grazing behavior shortly before their death, from the Proto-Aurignacian to the Early Aurignacian. During the Early Aurignacian, *R. tarandus* presents anisotropy values even higher than *E. ferus*, with all other DMTA parameters equal (Table 5). This reflects an even more abrasive diet for reindeer. These results demonstrate the local predominance of open landscapes, where the animals were hunted (Fig. 7). It is worth noting that the progressive landscape opening between Proto-Aurignacian and Early Aurignacian highlighted by bone collagen and enamel isotope analysis (Tables 3 and 4) and pollen analyses (Leroi-Gourhan, 1959; Fourcade et al., 2022) is not reflected by DMTA results. As mentioned in Berlioz et al. (2023), we interpret these results as indicating that Aurignacian groups from Isturitz chose to hunt their prey preferentially in open areas, regardless of how open the environment was.

Furthermore, the abrasive diet of reindeer shown by the DMTA does not support a winter diet mainly based on lichens (Rivals and Solounias, 2007). At least for reindeer, these results would support seasonal hunting, mainly during the 'good season' in July–August whenever the herbaceous layer is accessible in abundance, as also suggested by Rendu et al. (2017) based on the cementochronology of reindeer (analysis performed only for Intermediate and Early Aurignacian archaeostratigraphic units) and Bouchud (1966) based on reindeer tooth eruption. However, this finding cannot be generalized to the entire archaeological assemblage as archaeozoological analyses (Soulier, 2013; Soulier et al., 2014) have shown (notably through the presence of fetuses) that some horses, bison, and reindeer were also killed outside of the summer season.

5. Conclusions

The three complementary analytical techniques applied to the osteodental elements of the macromammals hunted and consumed by Isturitz human groups allowed us to better understand their ecosystem through their life, from their earlier years to the last weeks before their death, providing a direct relationship with the climatic and environmental conditions Aurignacian groups faced at the arrival to southwestern Europe. It provides an in-depth and comprehensive insight into the ecological setting exploited by the first Aurignacian groups of this region. The study reveals a context of marked climatic cooling and aridification between the Proto-Aurignacian and the Early Aurignacian, which is associated with a gradual environment opening, as revealed by the proxies analyzed and the available ones, such as pollen. Our findings suggest that those human populations occupied Isturitz under a cold and arid climate, which rapidly became even cooler and drier. However, this led only to limited changes in the procurement strategies and prey capture, underlining the stability of hunting strategies and adaptation abilities of these human populations despite the climatic changes. Indeed, sulfur analyses on animal bones testify to the use of a similar hunting territory near the cave throughout the temporal sequence. Although the proportion of other preyed ungulates varies, horses remain the primary animal resource hunted throughout the sequence. Irrespective of the significant environmental modifications induced by climate changes, the dental textures of the animals offer several avenues for reflection, favoring an almost systematic choice of human populations to hunt in open landscapes. Besides, the results obtained for reindeer reinforce the hypothesis of seasonal hunting, already supported by previous archaeozoological and cementochronological analyses. Our findings, therefore, reflect a consistent pattern of land and resource use in the ever-changing landscape of Isturitz despite the cooling and environmental aridification. This integrative methodological approach applied to the same animal specimens has proven to be relevant as a good instrument to reconstruct local climatic and environmental conditions on those animals accumulated by humans during the Early Upper Paleolithic.

Declaration of competing interest

All authors declare that they have contributed to this submission, and they have no known competing financial interests or personal relationships that could have appeared to influence the work reported in this paper.

Acknowledgments

This work has been supported by SUBSILIENCE (ID: ERC CoG Ref. 818299) and NEWINDS (Ref. PID2021-125818NB-I00) projects to A.B.M.-A.; EnvINExt (MSCA Ref. 101064818) to E.B and HOMEDSCAPE(PID2022-136832NB-100). We acknowledge the permission of Joëlle Darricau (owner of the archaeological site) and Olivier Ferullo (IE DRAC Nouvelle-Aquitaine) for promoting the research with the archaeological materials of Isturitz and providing study permissions. We want to thank Gabriele Terlato and Andrea Cicero Cabañas for assisting in sampling and laboratory processing. M.F.-G. is currently supported by an APOSTD postdoctoral fellowship (CIAPOS/2022/081), funded by the Generalitat Valenciana and the European Social Fund.

Author contributions

E. Berlioz: Writing – original draft, Validation, Software, Methodology, Investigation, Funding acquisition, Formal analysis, Data curation. **M. Fernández-García:** Writing – review & editing, Methodology, Formal analysis, Validation, Software, Investigation, Data curation. **M.-C. Soulier:** Writing – review & editing, Resources. **L. Agudo-Pérez:** Resources, Methodology, Formal analysis. **G. Amorós:** Formal analysis. **C. Normand:** Writing – review & editing, Resources, Investigation. **A.B. Marín-Arroyo:** Writing – review & editing, Validation, Supervision, Software, Resources, Project administration, Methodology, Investigation, Funding acquisition, Formal analysis, Data curation, Conceptualization.

Research data

All Supplementary Data (Tables S1–S6 and Supplementary Online Material [SOM1–SOM7]) mentioned in the study are available at: https://zenodo.org/records/15088619

References

Ambrose, S.H., 1990. Preparation and characterization of bone and tooth collagen for isotopic analysis. J. Archaeol. Sci. 17, 431–451.

Amundson, R., Austin, A.T., Schuur, E.A.G., Yoo, K., Matzek, V., Kendall, C., Uebersax, A., Brenner, D., Baisden, W.T., 2003. Global patterns of the isotopic composition of soil and plant nitrogen. Glob. Biogeochem. Cycles 17, 2002GB001903.

Bache, S.M., Wickham, H., Henry, L., Henry, M.L., 2022. Package 'magrittr.' R. Package Version.

Balasse, M., 2003. Potential biases in sampling design and interpretation of intra-tooth isotope analysis. Int. J. Osteoarchaeol. 13, 3–10.

Balasse, M., Smith, A.B., Ambrose, S.H., Leigh, S.R., 2003. Determining sheep birth seasonality by analysis of tooth enamel oxygen isotope ratios: The Late Stone Age site of Kasteelberg (South Africa). J. Archaeol. Sci. 30, 205–215.

Banks, W.E., 2017. The application of ecological niche modeling methods to archaeological data in order to examine culture-environment relationships and cultural trajectories. Quaternaire Rev. Assoc. Fr. Quatern. 28, 271–276.
Banks, W.E., d'Errico, F., Zilhão, J., 2013. Human–climate interaction during the Early Upper Paleolithic: Testing the hypothesis of an adaptive shift between the Proto-Aurignacian and the Early Aurignacian. J. Hum. Evol. 64, 39–55.
Barshay-Szmidt, C., Normand, C., Flas, D., Soulier, M.-C., 2018. Radiocarbon dating the Aurignacian sequence at Isturitz (France): Implications for the timing and development of the Protoaurignacian and Early Aurignacian in western Europe. J. Archaeol. Sci. Rep. 17, 809–838.
Bataille, C.P., Jaouen, K., Milano, S., Trost, M., Steinbrenner, S., Crubézy, É., Colleter, R., 2021. Triple sulfur-oxygen-strontium isotopes probabilistic geographic assignment of archaeological remains using a novel sulfur isoscape of western Europe. PLoS One 16, e0250383.
Ben-David, M., Flaherty, E.A., 2012. Stable isotopes in mammalian research: A beginner's guide. J. Mammal. 93, 312–328.
Berlioz, E., 2017. Écologie alimentaire et paléoenvironnements des cervidés européens du Pléistocène inférieur: le message des textures de micro-usure dentaire. Ph.D. Thesis. Université de Poitiers, France.
Berlioz, E., Azorit, C., Blondel, C., Tellado Ruiz, M.S., Merceron, G., 2017. Deer in an arid habitat: Dental microwear textures track feeding adaptability. Hystrix Ital. J. Mammal. 28, 222–230.
Berlioz, É., Kostopoulos, D.S., Blondel, C., Merceron, G., 2018. Feeding ecology of Eucladoceros ctenoides as a proxy to track regional environmental variations in Europe during the early Pleistocene. C.R. Palevol 17, 320–332.
Berlioz, E., Leduc, C., Hofman-Kamińska, E., Bignon-Lau, O., Kowalczyk, R., Merceron, G., 2022. Dental microwear foraging ecology of a large browsing ruminant in Northern Hemisphere: The European moose (*Alces alces*). Palaeogeogr. Palaeoclimatol. Palaeoecol. 586, 110754.
Berlioz, E., Capdepon, E., Discamps, E., 2023. A long-term perspective on Neanderthal environment and subsistence: Insights from the dental microwear texture analysis of hunted ungulates at Combe-Grenal (Dordogne, France). PLoS One 18, e0278395.
Bernard, A., Daux, V., Lécuyer, C., Brugal, J.-P., Genty, D., Wainer, K., Gardien, V., Fourel, F., Jaubert, J., 2009. Pleistocene seasonal temperature variations recorded in the $\delta^{18}O$ of *Bison priscus* teeth. Earth Planet. Sci. Lett. 283, 133–143.
Bignon-Lau, O., Catz, N., Berlioz, E., Veiberg, V., Strand, O., Merceron, G., 2017. Dental microwear textural analyses to track feeding ecology of reindeer: A comparison of two contrasting populations in Norway. Mammal Res. 62, 111–120.
Blumenthal, S.A., Cerling, T.E., Smiley, T.M., Badgley, C.E., Plummer, T.W., 2019. Isotopic records of climate seasonality in equid teeth. Geochem. Cosmochim. Acta 260, 329–348.
Bocherens, H., 2015. Isotopic tracking of large carnivore palaeoecology in the mammoth steppe. Quatern. Sci. Rev. 117, 42–71.
Bocherens, H., Argant, A., Argant, J., Billiou, D., Crégut-Bonnoure, E., Donat-Ayache, B., Philippe, M., Thinon, M., 2004. Diet reconstruction of ancient brown bears (*Ursus arctos*) from Mont Ventoux (France) using bone collagen stable isotope biogeochemistry (^{13}C, ^{15}N). Can. J. Zool. 82, 576–586.
Bocherens, H., Hofman-Kamińska, E., Drucker, D.G., Schmölcke, U., Kowalczyk, R., 2015. European bison as a refugee species? Evidence from isotopic data on Early Holocene bison and other large herbivores in northern Europe. PLoS One 10, e0115090.
Bojarska, K., Selva, N., 2012. Spatial patterns in brown bear *Ursus arctos* diet: The role of geographical and environmental factors. Mammal Rev. 42, 120–143.
Bonafini, M., Pellegrini, M., Ditchfield, P., Pollard, A.M., 2013. Investigation of the 'canopy effect' in the isotope ecology of temperate woodlands. J. Archaeol. Sci. 40, 3926–3935.
Bouchud, J., 1966. Essai sur le Renne et la climatologie du Paléolithique moyen et supérieur. Ph.D. Thesis. Université de Paris, France.
Bowen, G.J., Wilkinson, B., 2002. Spatial distribution of $\delta^{18}O$ in meteoric precipitation. Geology 30, 315–318.
Britton, K., Jimenez, E.-L., Le Corre, M., Pederzani, S., Daujeard, C., Jaouen, K., Vettese, D., Tütken, T., Hublin, J.-J., Moncel, M.-H., 2023. Multi-isotope zooarchaeological investigations at Abri du Maras: The paleoecological and paleoenvironmental context of Neanderthal subsistence strategies in the Rhône Valley during MIS 3. J. Hum. Evol. 174, 103292.
Bronk Ramsey, C., 2021. OxCal v4. 4.4. Retrieved from: https://c14.arch.ox.ac.uk/oxcal.html.
Brown, T.A., Nelson, D.E., Vogel, J.S., Southon, J.R., 1988. Improved collagen extraction by modified Longin method. Radiocarbon 30, 171–177.
Bryant, J.D., Luz, B., Froelich, P.N., 1994. Oxygen isotopic composition of fossil horse tooth phosphate as a record of continental paleoclimate. Palaeogeogr. Palaeoclimatol. Palaeoecol. 107, 303–316.
Calandra, I., Merceron, G., 2016. Dental microwear texture analysis in mammalian ecology. Mammal Rev. 46, 215–228.
Calandra, I., Zub, K., Szafrańska, P.A., Zalewski, A., Merceron, G., 2016. Silicon-based plant defences, tooth wear and voles. J. Exp. Biol. 219, 501–507.
Cerling, T.E., Harris, J.M., 1999. Carbon isotope fractionation between diet and bioapatite in ungulate mammals and implications for ecological and paleoecological studies. Oecologia 120, 347–363.
Chillón, B.S., Alberdi, M.T., Leone, G., Bonadonna, F.P., Stenni, B., Longinelli, A., 1994. Oxygen isotopic composition of fossil equid tooth and bone phosphate: An archive of difficult interpretation. Palaeogeogr. Palaeoclimatol. Palaeoecol. 107, 317–328.
Clementz, M.T., 2012. New insight from old bones: Stable isotope analysis of fossil mammals. J. Mammal. 93, 368–380.
Conover, W.J., Iman, R.L., 1981. Rank transformations as a bridge between parametric and nonparametric statistics. Am. Statistician 35, 124–129.
Costamagno, S., 2017. Taphonomie et archéozoologie des ensembles fauniques aurignaciens d'Isturitz. In: Actes de La Table Ronde Du Cinquantenaire Du Classement Comme Monument Historique Des Grottes d'Isturitz et d'Oxocelhaya. Presented at the La grotte d'Isturitz. Fouilles anciennes et récentes, Cédarc, pp. 191–204.
Craine, J.M., Elmore, A.J., Aidar, M.P.M., Bustamante, M., Dawson, T.E., Hobbie, E.A., Kahmen, A., Mack, M.C., McLauchlan, K.K., Michelsen, A., Nardoto, G.B., Pardo, L.H., Peñuelas, J., Reich, P.B., Schuur, E.A.G., Stock, W.D., Templer, P.H., Virginia, R.A., Welker, J.M., Wright, I.J., 2009. Global patterns of foliar nitrogen isotopes and their relationships with climate, mycorrhizal fungi, foliar nutrient concentrations, and nitrogen availability. New Phytol. 183, 980–992.
Dag, O., Dolgun, A., Konar, N.M., 2018. Onewaytests: An R package for one-way tests in independent groups designs. R J. 10.
D'Angela, D., Longinelli, A., 1990. Oxygen isotopes in living mammal's bone phosphate: Further results. Chem. Geol. Isot. Geosci. 86, 75–82.
Dansgaard, W., 1964. Stable isotopes in precipitation. Tellus 16, 436–468.
De Saint-Périer, R., 1935. Quelques oeuvres d'art de la grotte d'Isturitz. Bull. Soc. Préhist. Fr. 32, 64–77.
DeNiro, M.J., 1985. Postmortem preservation and alteration of in vivo bone collagen isotope ratios in relation to palaeodietary reconstruction. Nature 317, 806–809.
DeSantis, L.R., 2016. Dental microwear textures: Reconstructing diets of fossil mammals. Surf. Topogr. Metrol. Prop. 4, 1–12.
Discamps, E., Jaubert, J., Bachellerie, F., 2011. Human choices and environmental constraints: Deciphering the variability of large game procurement from Mousterian to Aurignacian times (MIS 5-3) in southwestern France. Quatern. Sci. Rev. 30, 2755–2775.
Drucker, D., Bocherens, H., Pike-Tay, A., Mariotti, A., 2001. Isotopic tracking of seasonal dietary change in dentine collagen: Preliminary data from modern caribou. C.R. Acad. Sci. Ser. IIA Earth Planet. Sci. 333, 303–309.
Drucker, D.G., Bocherens, H., Billiou, D., 2003. Evidence for shifting environmental conditions in Southwestern France from 33 000 to 15 000 years ago derived from carbon-13 and nitrogen-15 natural abundances in collagen of large herbivores. Earth Planet. Sci. Lett. 216, 163–173.
Drucker, D.G., Rivals, F., Nadal, J., Ruffí, I., Soler, J., Soler, N., Maroto, J., 2024. Ecology of large ungulates in the northeastern Iberian Peninsula during the Upper Palaeolithic through stable isotopes and tooth wear analysis. Quatern. Environ. Humans, 100011.
Drucker, D.G., Bridault, A., Hobson, K.A., Szuma, E., Bocherens, H., 2008. Can carbon-13 in large herbivores reflect the canopy effect in temperate and boreal ecosystems? Evidence from modern and ancient ungulates. Palaeogeogr. Palaeoclimatol. Palaeoecol. 266, 69–82.
Fernández-García, M., Vidal-Cordasco, M., Jones, J.R., Marín-Arroyo, A.B., 2023. Reassessing palaeoenvironmental conditions during the Middle to Upper Palaeolithic transition in the Cantabrian region (Southwestern Europe). Quatern. Sci. Rev. 301, 107928.
Fernández-García, M., Pederzani, S., Britton, K., Agudo-Pérez, L., Cicero, A., Geiling, J.M., Daura, J., Sanz, M., Marín-Arroyo, A.B., 2024. Palaeoecology of ungulates in northern Iberia during the Late Pleistocene through isotopic analysis of teeth. Biogeosciences 21, 4413–4437.
Fick, S.E., Hijmans, R.J., 2017. WorldClim 2: New 1-km spatial resolution climate surfaces for global land areas. Int. J. Climatol. 37, 4302–4315.
Fourcade, T., Sánchez Goñi, M.F.S., Lahaye, C., Rossignol, L., Philippe, A., 2022. Environmental changes in SW France during the Middle to Upper Paleolithic transition from the pollen analysis of an eastern North Atlantic deep-sea core. Quatern. Res. 110, 147–164.
Francisco, A., Blondel, C., Brunetière, N., Ramdarshan, A., Merceron, G., 2018a. Enamel surface topography analysis for diet discrimination. A methodology to enhance and select discriminative parameters. Surf. Topogr. Metrol. Prop. 6, 015002.
Francisco, A., Brunetière, N., Merceron, G., 2018b. Gathering and analyzing surface parameters for diet identification purposes. Technologies 6, 75.
Geist, V., 1998. Deer of the World: Their Evolution, Behaviour, and Ecology. Stackpole Books.
Gibbard, P., Cohen, K.M., 2008. Global chronostratigraphical correlation table for the last 2.7 million years. Episodes 31, 243–247.
Grine, F.E., 1986. Dental evidence for dietary differences in *Australopithecus* and *Paranthropus*: A quantitative analysis of permanent molar microwear. J. Hum. Evol. 15, 783–822.
Guthrie, R.D., 1990. Frozen fauna of the mammoth steppe: The story of Blue Babe. In: Frozen Fauna of the Mammoth Steppe. University of Chicago Press.
Hajdinjak, M., Mafessoni, F., Skov, L., Vernot, B., Hübner, A., Fu, Q., Essel, E., Nagel, S., Nickel, B., Richter, J., 2021. Initial Upper Palaeolithic humans in Europe had recent Neanderthal ancestry. Nature 592, 253–257.
Harrell Jr., F.E., Harrell Jr., M.F.E., 2019. Package 'hmisc.' CRAN2018, 2019, pp. 235–236.
Hedges, R.E., Clement, J.G., Thomas, C.D.L., O'connell, T.C., 2007. Collagen turnover in the adult femoral mid-shaft: Modeled from anthropogenic radiocarbon tracer measurements. Am. J. Phys. Anthropol. Off. Publ. Am. Assoc. Phys. Anthropol. 133, 808–816.
Helmer, D., Monchot, H., 2006. Un site mésolithique de chasse à l'aurochs (La Montagne, Sénas, Bouches-du-Rhône). Anthropozoologica 41, 215–228.
Hermier, R., Merceron, G., Kostopoulos, D.S., 2020. The emblematic Eurasian Villafranchian antelope *Gazellospira* (Mammalia: Bovidae): New insights from the Lower Pleistocene Dafnero fossil sites (Northern Greece). Geobios 61, 11–29.

Hoppe, K.A., 2006. Correlation between the oxygen isotope ratio of North American bison teeth and local waters: Implication for paleoclimatic reconstructions. Earth Planet. Sci. Lett. 244, 408–417.
Hoppe, K.A., Stover, S.M., Pascoe, J.R., Amundson, R., 2004. Tooth enamel biomineralization in extant horses: Implications for isotopic microsampling. Palaeogeogr. Palaeoclimatol. Palaeoecol. 206, 355–365.
Hublin, J.-J., Sirakov, N., Aldeias, V., Bailey, S., Bard, E., Delvigne, V., Endarova, E., Fagault, Y., Fewlass, H., Hajdinjak, M., 2020. Initial upper palaeolithic *Homo sapiens* from Bacho Kiro cave, Bulgaria. Nature 581, 299–302.
Huertas, A.D., Iacumin, P., Stenni, B., Chillón, B.S., Longinelli, A., 1995. Oxygen isotope variations of phosphate in mammalian bone and tooth enamel. Geochem. Cosmochim. Acta 59, 4299–4305.
Hullot, M., Antoine, P.-O., Ballatore, M., Merceron, G., 2019. Dental microwear textures and dietary preferences of extant rhinoceroses (Perissodactyla, Mammalia). Mammal Res. 64, 397–409.
Iasi, L.N.M., Chintalapati, M., Skov, L., Bossoma Mesa, A., Hajdinjak, M., Peter, B.M., Moorjani, P., 2024. Neandertal ancestry through time: Insights from genomes of ancient and present-day humans. bioRxiv, 2024–05.
Jones, J.R., Richards, M.P., Straus, L.G., Reade, H., Altuna, J., Mariezkurrena, K., Marín-Arroyo, A.B., 2018. Changing environments during the Middle-Upper Palaeolithic transition in the eastern Cantabrian Region (Spain): Direct evidence from stable isotope studies on ungulate bones. Sci. Rep. 8, 1–20.
Jones, J.R., Richards, M.P., Reade, H., de Quirós, F.B., Marín-Arroyo, A.B., 2019. Multi-Isotope investigations of ungulate bones and teeth from El Castillo and Covalejos caves (Cantabria, Spain): Implications for paleoenvironment reconstructions across the Middle-Upper Palaeolithic transition. J. Archaeol. Sci. Rep. 23, 1029–1042.
Jones, J.R., Marín-Arroyo, A.B., Rodríguez, M.C., Richards, M.P., 2021. After the Last Glacial Maximum in the refugium of northern Iberia: Environmental shifts, demographic pressure and changing economic strategies at Las Caldas Cave (Asturias, Spain). Quatern. Sci. Rev. 262, 106931.
Kassambara, A., 2023. ggpubr: "ggplot2" Based Publication Ready Plots.
Kohn, M.J., 2004. Comment: Tooth enamel mineralization in ungulates: Implications for recovering a primary isotopic time-series, by BH Passey and TE Cerling (2002). Geochem. Cosmochim. Acta 68, 403–405.
Lécuyer, C., Hillaire-Marcel, C., Burke, A., Julien, M.-A., Hélie, J.-F., 2021. Temperature and precipitation regime in LGM human refugia of southwestern Europe inferred from $\delta^{13}C$ and $\delta^{18}O$ of large mammal remains. Quatern. Sci. Rev. 255, 106796.
Lenoble, A., Texier, J.-P., 2016. Processus géologiques de formation du site d'Isturitz (Sud-Ouest de la France). Implications archéologiques. Paleo Rev. Archéol. Préhist. 235–252.
Leroi-Gourhan, A., 1959. Résultats de l'analyse pollinique de la grotte d'Isturitz. Bull. Soc. Préhist. Fr. 56, 619–624.
Lisiecki, L.E., Raymo, M.E., 2005. A Pliocene-Pleistocene stack of 57 globally distributed benthic $\delta^{18}O$ records. Paleoceanography 20, 1–17.
Liu, X., Wang, G., Li, J., Wang, Q., 2010. Nitrogen isotope composition characteristics of modern plants and their variations along an altitudinal gradient in Dongling Mountain in Beijing. Sci. China Ser. D Earth Sci. 53, 128–140.
Männel, T.T., Auerswald, K., Schnyder, H., 2007. Altitudinal gradients of grassland carbon and nitrogen isotope composition are recorded in the hair of grazers. Glob. Ecol. Biogeogr. 16, 583–592.
Mellars, P., 2006. Archaeology and the dispersal of modern humans in Europe: Deconstructing the "Aurignacian.". Evol. Anthropol. 15, 167–182.
Merceron, G., Escarguel, G., Angibault, J.-M., Verheyden-Tixier, H., 2010. Can dental microwear textures record inter-individual dietary variations? PLoS One 5, 1–9.
Merceron, G., Hofman-Kamińska, E., Kowalczyk, R., 2014. 3D dental microwear texture analysis of feeding habits of sympatric ruminants in the Białowieża Primeval Forest, Poland. For. Ecol. Manag. 328, 262–269.
Merceron, G., Berlioz, E., Vonhof, H., Green, D., Garel, M., Tütken, T., 2021. Tooth tales told by dental diet proxies: An alpine community of sympatric ruminants as a model to decipher the ecology of fossil fauna. Palaeogeogr. Palaeoclimatol. Palaeoecol. 562, 110077.
Merceron, G., Madelaine, S., 2006. Molar microwear pattern and palaeoecology of ungulates from La Berbie (Dordogne, France): Environment of Neanderthals and modern human populations of the Middle/Upper Palaeolithic. Boreas 35, 272–278.
Merceron, G., Ungar, P., 2005. Dental microwear and palaeoecology of bovids from the Early Pliocene of Langebaanweg, Western Cape province, South Africa. S. Afr. J. Sci. 101, 365–370.
Merceron, G., Schulz, E., Kordos, L., Kaiser, T.M., 2007. Paleoenvironment of *Dryopithecus brancoi* at Rudabánya, Hungary: Evidence from dental meso- and micro-wear analyses of large vegetarian mammals. J. Hum. Evol. 53, 331–349.
Merceron, G., Ramdarshan, A., Blondel, C., Boisserie, J.-R., Brunetiere, N., Francisco, A., Gautier, D., Milhet, X., Novello, A., Pret, D., 2016. Untangling the environmental from the dietary: Dust does not matter. Proc. R. Soc. B 283, 1–8.
Micó, C., Blasco, R., Muñoz Del Pozo, A., Jiménez-García, B., Rosell, J., Rivals, F., 2024a. Differentiating taphonomic features from trampling and dietary microwear, an experimental approach. Historical Biol. 36, 760–782.
Micó, C., Blasco, R., Rivals, F., 2024b. Simulating taphonomic processes on teeth: The impact of sediment pressure and thermal alteration on dental microwear. Quatern. Sci. Adv. 14, 100195.
Mylopotamitaki, D., Weiss, M., Fewlass, H., Zavala, E.I., Rougier, H., Sümer, A.P., Hajdinjak, M., Smith, G.M., Ruebens, K., Sinet-Mathiot, V., Pederzani, S., Essel, E., Harking, F.S., Xia, H., Hansen, J., Kirchner, A., Lauer, T., Stahlschmidt, M., Hein, M., Talamo, S., Wacker, L., Meller, H., Dietl, H., Orschiedt, J., Olsen, J.V., Zeberg, H., Prüfer, K., Krause, J., Meyer, M., Welker, F., McPherron, S.P., Schüler, T., Hublin, J.-J., 2024. *Homo sapiens* reached the higher latitudes of Europe by 45,000 years ago. Nature 626, 341–346.
Naito, Y.I., Meleg, I.N., Robu, M., Vlaicu, M., Drucker, D.G., Wißing, C., Hofreiter, M., Barlow, A., Bocherens, H., 2020. Heavy reliance on plants for Romanian cave bears evidenced by amino acid nitrogen isotope analysis. Sci. Rep. 10, 6612.
Nehlich, O., 2015. The application of sulphur isotope analyses in archaeological research: A review. Earth Sci. Rev. 142, 1–17.
Nehlich, O., Richards, M.P., 2009. Establishing collagen quality criteria for sulphur isotope analysis of archaeological bone collagen. Archaeol. Anthropol. Sci. 1, 59–75.
Noe-Nygaard, N., Price, T.D., Hede, S.U., 2005. Diet of aurochs and early cattle in southern Scandinavia: Evidence from 15N and 13C stable isotopes. J. Archaeol. Sci. 32, 855–871.
Normand, C., 2005. Les occupations aurignaciennes de la grotte d'Isturitz (Saint-Martin-d'Arberoue, Pyrénées-Atlantiques, France): Synthèse des données actuelles. Munibe Antropol. Arkeol. 119–129.
Normand, C., 2017. La grotte d'Isturitz: Présentation. In: Actes de La Table Ronde Du Cinquantenaire Du Classement Comme Monument Historique Des Grottes d'Isturitz et d'Oxocelhaya. Presented at the La grotte d'Isturitz. Fouilles anciennes et récentes, Cedarc, pp. 9–24.
Normand, C., de Beaune, S.A., Costamagno, S., Diot, M.-F., Henry-Gambier, D., Goutas, N., Laroulandie, V., Lenoble, A., O'Farrell, M., Rendu, W., 2007. Nouvelles données sur la séquence aurignacienne de la grotte d'Isturitz (communes d'Isturitz et de Saint-Martin-d'Arberoue. Pyrénées-Atlantiques). In: Actes Du Congrès Préhistorique de France. Presented at the XXVIe session, Congrès du Centenaire, Mémoires de la Société préhistorique française, Avignon, pp. 277–293.
Orlandi-Oliveras, G., Köhler, M., Clavel, J., Scott, R., Mayda, S., Kaya, T., Merceron, G., 2022. Feeding strategies of circum-Mediterranean hipparionins during the late Miocene: Exploring dietary preferences related to size through dental microwear analysis. Palaeontol. Electron. 1–45.
Pacher, M., Stuart, A.J., 2009. Extinction chronology and palaeobiology of the cave bear (*Ursus spelaeus*). Boreas 38, 189–206.
Palmqvist, P., Gröcke, D.R., Arribas, A., Fariña, R.A., 2003. Paleoecological reconstruction of a lower Pleistocene large mammal community using biogeochemical ($\delta^{13}C$, $\delta^{15}N$, $\delta^{18}O$, Sr:Zn) and ecomorphological approaches. Paleobiology 29, 205–229.
Passemard, E., 1913. Fouilles à Isturitz (Basses-Pyrénées). Bull. Soc. Préhist. Fr. 10, 647–649.
Pederzani, S., Britton, K., 2019. Oxygen isotopes in bioarchaeology: Principles and applications, challenges and opportunities. Earth Sci. Rev. 188, 77–107.
Pederzani, S., Aldeias, V., Dibble, H.L., Goldberg, P., Hublin, J.-J., Madelaine, S., McPherron, S.P., Sandgathe, D., Steele, T.E., Turq, A., 2021. Reconstructing Late Pleistocene paleoclimate at the scale of human behavior: An example from the Neandertal occupation of La Ferrassie (France). Sci. Rep. 11, 1419.
Pederzani, S., Britton, K., Jones, J.R., Pérez, L.A., Geiling, J.M., Marín-Arroyo, A.B., 2023. Late Pleistocene Neanderthal exploitation of stable and mosaic ecosystems in northern Iberia shown by multi-isotope evidence. Quatern. Res. 1–25.
Pellegrini, M., Snoeck, C., 2016. Comparing bioapatite carbonate pre-treatments for isotopic measurements: Part 2—Impact on carbon and oxygen isotope compositions. Chem. Geol. 420, 88–96.
Prüfer, K., Posth, C., Yu, H., Stoessel, A., Spyrou, M.A., Deviese, T., Mattonai, M., Ribechini, E., Higham, T., Velemínskỳ, P., 2021. A genome sequence from a modern human skull over 45,000 years old from Zlatỳ kůň in Czechia. Nature Ecol. Evol. 5, 820–825.
Pryor, A.J., Stevens, R.E., O'Connell, T.C., Lister, J.R., 2014. Quantification and propagation of errors when converting vertebrate biomineral oxygen isotope data to temperature for palaeoclimate reconstruction. Palaeogeogr. Palaeoclimatol. Palaeoecol. 412, 99–107.
Rasmussen, S.O., Bigler, M., Blockley, S.P., Blunier, T., Buchardt, S.L., Clausen, H.B., Cvijanovic, I., Dahl-Jensen, D., Johnsen, S.J., Fischer, H., 2014. A stratigraphic framework for abrupt climatic changes during the Last Glacial period based on three synchronized Greenland ice-core records: Refining and extending the INTIMATE event stratigraphy. Quatern. Sci. Rev. 106, 14–28.
Ramdarshan, A., Blondel, C., Gautier, D., Surault, J., Merceron, G., 2017. Overcoming sampling issues in dental tribology: Insights from an experimentation on sheep. Palaeontogr. Electron. 20, 1–19.
Reade, H., Tripp, J.A., Frémondeau, D., Sayle, K.L., Higham, T.F., Street, M., Stevens, R.E., 2023. Nitrogen palaeo-isoscapes: Changing spatial gradients of faunal $\delta^{15}N$ in late Pleistocene and early Holocene Europe. PLoS One 18, e0268607.
Reimer, P.J., Bard, E., Bayliss, A., Beck, J.W., Blackwell, P.G., Ramsey, C.B., Buck, C.E., Cheng, H., Edwards, R.L., Friedrich, M., 2013. IntCal13 and Marine13 radiocarbon age calibration curves 0–50,000 years cal BP. Radiocarbon 55, 1869–1887.
Reimer, P.J., Austin, W.E., Bard, E., Bayliss, A., Blackwell, P.G., Ramsey, C.B., Butzin, M., Cheng, H., Edwards, R.L., Friedrich, M., 2020. The IntCal20 Northern Hemisphere radiocarbon age calibration curve (0–55 cal kBP). Radiocarbon 62, 725–757.
Rendu, W., Soulier, M.-C., Pubert, E., Costamagno, S., Normand, C., 2017. Saisonnalité des activités de prédation des chasseurs aurignaciens d'Isturitz. In: Actes de La Table Ronde Du Cinquantenaire Du Classement Comme Monument Historique Des Grottes d'Isturitz et d'Oxocelhaya. Presented at the La grotte d'Isturitz. Fouilles anciennes et récentes, Cédarc.
Rey, K., Amiot, R., Lécuyer, C., Koufos, G.D., Martineau, F., Fourel, F., Kostopoulos, D.S., Merceron, G., 2013. Late Miocene climatic and environmental variations in northern Greece inferred from stable isotope compositions ($\delta^{18}O$, $\delta^{13}C$) of equid teeth apatite. Palaeogeogr. Palaeoclimatol. Palaeoecol. 388, 48–57.

Richards, M.P., Hedges, R.E., 1999. Stable isotope evidence for similarities in the types of marine foods used by Late Mesolithic humans at sites along the Atlantic coast of Europe. J. Archaeol. Sci. 26, 717–722.
Richards, M.P., Fuller, B.T., Sponheimer, M., Robinson, T., Ayliffe, L., 2003. Sulphur isotopes in palaeodietary studies: A review and results from a controlled feeding experiment. Int. J. Osteoarchaeol. 13, 37–45.
Rivals, F., Solounias, N., 2007. Differences in tooth microwear of populations of caribou (*Rangifer tarandus*, Ruminantia, Mammalia) and implications to ecology, migration, glaciations and dental evolution. J. Mammal. Evol. 14, 182.
Rivals, F., Álvarez-Lao, D.J., 2018. Ungulate dietary traits and plasticity in zones of ecological transition inferred from late Pleistocene assemblages at Jou Puerta and Rexidora in the Cantabrian Region of northern Spain. Palaeogeogr. Palaeoclimatol. Palaeoecol. 499, 123–130.
Sánchez Goñi, M.F., Harrison, S.P., 2010. Millennial-scale climate variability and vegetation changes during the Last Glacial: Concepts and terminology. Quatern. Sci. Rev. 29, 2823–2827.
Sánchez Goñi, M.F.S., Landais, A., Fletcher, W.J., Naughton, F., Desprat, S., Duprat, J., 2008. Contrasting impacts of Dansgaard–Oeschger events over a western European latitudinal transect modulated by orbital parameters. Quatern. Sci. Rev. 27, 1136–1151.
Sankararaman, S., Patterson, N., Li, H., Pääbo, S., Reich, D., 2012. The date of interbreeding between Neandertals and modern humans. PLoS Genet 8, e1002947. https://doi.org/10.1371/journal.pgen.1002947.
Schubert, B.W., Ungar, P.S., Sponheimer, M., Reed, K.E., 2006. Microwear evidence for Plio-Pleistocene bovid diets from Makapansgat Limeworks Cave, South Africa. Palaeogeogr. Palaeoclimatol. Palaeoecol. 241, 301–319.
Schulz, E., Piotrowski, V., Clauss, M., Mau, M., Merceron, G., Kaiser, T.M., 2013. Dietary abrasiveness is associated with variability of microwear and dental surface texture in rabbits. PLoS One 8, 1–7.
Scott, J.R., 2012. Dental microwear texture analysis of extant African Bovidae. Mammalia 76, 157–174.
Scott, R.S., Ungar, P.S., Bergstrom, T.S., Brown, C.A., Grine, F.E., Teaford, M.F., Walker, A., 2005. Dental microwear texture analysis shows within-species diet variability in fossil hominins. Nature 436, 693–695.
Scott, R.S., Ungar, P.S., Bergstrom, T.S., Brown, C.A., Childs, B.E., Teaford, M.F., Walker, A., 2006. Dental microwear texture analysis: Technical considerations. J. Hum. Evol. 51, 339–349.
Scott, J.R., Godfrey, L.R., Jungers, W.L., Scott, R.S., Simons, E.L., Teaford, M.F., Ungar, P.S., Walker, A., 2009. Dental microwear texture analysis of two families of subfossil lemurs from Madagascar. J. Hum. Evol. 56, 405–416.
Scott, R.S., Teaford, M.F., Ungar, P.S., 2012. Dental microwear texture and anthropoid diets. Am. J. Phys. Anthropol. 147, 551–579.
Slimak, L., Zanolli, C., Higham, T., Frouin, M., Schwenninger, J.-L., Arnold, L.J., Demuro, M., Douka, K., Mercier, N., Guérin, G., 2022. Modern human incursion into Neanderthal territories 54,000 years ago at Mandrin, France. Sci. Adv. 8, eabj9496.
Slon, V., Mafessoni, F., Vernot, B., De Filippo, C., Grote, S., Viola, B., Hajdinjak, M., Peyrégne, S., Nagel, S., Brown, S., 2018. The genome of the offspring of a Neanderthal mother and a Denisovan father. Nature 561, 113–116.
Snoeck, C., Pellegrini, M., 2015. Comparing bioapatite carbonate pre-treatments for isotopic measurements: Part 1—Impact on structure and chemical composition. Chem. Geol. 417, 394–403.
Soulier, M.C., 2013. Entre alimentaire et technique: l'exploitation animale aux débuts du paléolithique supérieur: stratégies de subsistance et chaînes opératoires de traitement du gibier à Isturitz, La Quina aval, Roc-de-Combe et Les Abeilles. Univ. Toulouse 2, Le Mirail.
Soulier, M.C., Goutas, N., Normand, C., Legrand, A., White, R.G., 2014. Regards croisés de l'archéozoologue et du technologue sur l'exploitation des ressources animales à l'Aurignacien archaïque. In: Transitions, Ruptures et Continuité En Préhistoire. Presented at the XXVIIe congrès préhistorique de France, Bordeaux - Les Eyzies.
Stuart, A.J., 1991. Mammalian extinctions in the Late Pleistocene of northern Eurasia and North America. Biol. Rev. 66, 453–562.
Tarriño, A., Normand, C., 2002. Procedencia de los restos líticos en el Auriñaciense antiguo (C 4b1) de Isturitz (Pyrénées-Atlantiques, Francia). Espac. Tiempo Forma Ser. I Prehist. Arqueol. 135–143.
Teaford, M.F., Oyen, O.J., 1989. In vivo and in vitro turnover in dental microwear. Am. J. Phys. Anthropol. 80, 447–460.
Teaford, M.F., Glander, K.E., 1991. Dental microwear in live, wild-trapped *Alouatta palliata* from Costa Rica. Am. J. Phys. Anthropol. 85, 313–319.
Tejada-Lara, J.V., MacFadden, B.J., Bermudez, L., Rojas, G., Salas-Gismondi, R., Flynn, J.J., 2018. Body mass predicts isotope enrichment in herbivorous mammals. Proc. R. Soc. B 285, 20181020.
Torres-Iglesias, L., Marín-Arroyo, A.B., Welker, F., de la Rasilla, M., 2024. Using ZooMS to assess archaeozoological insights and unravel human subsistence behaviour at La Viña rock shelter (northern Iberia). J. Archaeol. Sci. 161, 105904.
Ungar, P.S., 2015. Mammalian dental function and wear: A review. Biosurf. Biotribol. 1, 25–41.
Ungar, P.S., Merceron, G., Scott, R.S., 2007. Dental microwear texture analysis of Varswater bovids and early Pliocene paleoenvironments of Langebaanweg, Western Cape Province, South Africa. J. Mamm. Evol. 14, 163–181.
Van Klinken, G.J., 1999. Bone collagen quality indicators for palaeodietary and radiocarbon measurements. J. Archaeol. Sci. 26, 687–695.
Van Vuure, C., 2005. Retracing the aurochs. In: Neue Modelle Zu Masznahmen Der Landschaftsentwicklung Mit Groszen Pflanzenfressern Und Praktische Erfahrungen Bei Der Umsetzung, pp. 261–265.
Vidal-Cordasco, M., Ocio, D., Hickler, T., Marín-Arroyo, A.B., 2022. Ecosystem productivity affected the spatiotemporal disappearance of Neanderthals in Iberia. Nat. Ecol. Evol. 6, 1644–1657.
Vidal-Cordasco, M., Terlato, G., Ocio, D., Marín-Arroyo, A.B., 2023. Neanderthal coexistence with *Homo sapiens* in Europe was affected by herbivore carrying capacity. Sci. Adv. 9, eadi4099.
Weber, K., Winkler, D.E., Schulz-Kornas, E., Kaiser, T.M., Tütken, T., 2022. Post-mortem enamel surface texture alteration during taphonomic processes—Do experimental approaches reflect natural phenomena? PeerJ 10, e12635.
Wei, T., Simko, V.R., Levy, M., 2021. Package "corrplot": Visualization of a Correlation Matrix. 2017, Version 0.84.
White, R., Normand, C., 2015. Les parures de l'Aurignacien ancien et archaïque de la grotte d'Isturitz: perspectives technologiques et régionales with the collaboration of Bon, F.R. White, R. Bourrillon (Eds.), Aurignacian Genius: Art, Technologie et Société des Premiers Hommes Modernes en Europe, Actes du symposium international, 8–10 April 2013, New York University. Palethnologie 7 (2015), pp. 140–166.
Wickham, H., Chang, W., Wickham, M.H., 2016. Package 'ggplot2.' Create elegant data visualisations using the grammar of graphics, Version. 2, pp. 1–189.
Winkler, D.E., Schulz-Kornas, E., Kaiser, T.M., Codron, D., Leichliter, J., Hummel, J., Martin, L.F., Clauss, M., Tütken, T., 2020. The turnover of dental microwear texture: Testing the "last supper" effect in small mammals in a controlled feeding experiment. Palaeogeogr. Palaeoclimatol. Palaeoecol. 557, 109930.
Wolff, E.W., Chappellaz, J., Blunier, T., Rasmussen, S.O., Svensson, A., 2010. Millennial-scale variability during the last glacial: The ice core record. Quatern. Sci. Rev. 29, 2828–2838.
Wright, E., 2013. The history of the European aurochs (*Bos primigenius*) from the Middle Pleistocene to its extinction: An archaeological investigation of its evolution, morphological variability and response to human exploitation. Ph.D. Thesis. University of Sheffield.
Xafis, A., Nagel, D., Bastl, K., 2017. Which tooth to sample? A methodological study of the utility of premolar/non-carnassial teeth in the microwear analysis of mammals. Palaeogeogr. Palaeoclimatol. Palaeoecol. 487, 229–240.
Zazzo, A., Bendrey, R., Vella, D., Moloney, A.P., Monahan, F.J., Schmidt, O., 2012. A refined sampling strategy for intra-tooth stable isotope analysis of mammalian enamel. Geochem. Cosmochim. Acta 84, 1–13.
Zuur, A.F., Ieno, E.N., Elphick, C.S., 2010. A protocol for data exploration to avoid common statistical problems. Methods Ecol. Evol. 1, 3–14.